Accepted Manuscript

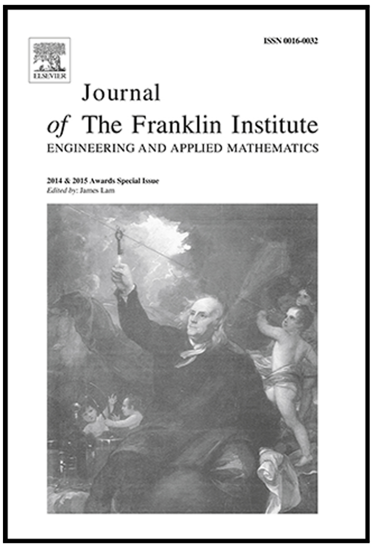

Mixed Rectilinear Sources Localization Under Unknown Mutual Coupling

Hua Chen, Wei Liu, Wei-Ping Zhu, M.N.S. Swamy, Qing Wang

PII: S0016-0032(19)30048-1
DOI: https://doi.org/10.1016/j.jfranklin.2019.01.019
Reference: FI 3755

To appear in: *Journal of the Franklin Institute*

Received date: 29 August 2018
Revised date: 3 December 2018
Accepted date: 12 January 2019

Please cite this article as: Hua Chen, Wei Liu, Wei-Ping Zhu, M.N.S. Swamy, Qing Wang, Mixed Rectilinear Sources Localization Under Unknown Mutual Coupling, *Journal of the Franklin Institute* (2019), doi: https://doi.org/10.1016/j.jfranklin.2019.01.019

Mixed Rectilinear Sources Localization Under Unknown Mutual Coupling

Hua Chen[a], Wei Liu[b], Wei-Ping Zhu[c], M.N.S. Swamy[c], Qing Wang[d]

[a]*Faculty of Information Science and Engineering, Ningbo University, Ningbo 315211,P. R. China.*
[b]*Department of Electronic and Electrical Engineering, The University of Sheffield, Sheffield S1 3JD, UK.*
[c]*Department of Electrical and Computer Engineering, Concordia University, Montreal, QC H3G 1M8, Canada.*
[d]*School of Electronic Informatin Engineering, Tianjin University, Tianjin 300072, P. R. China.*

Abstract

In this paper, a novel rectilinearity-based localization method for mixed near-field (NF) and far-field (FF) sources is proposed under unknown mutual coupling. The multiple parameters including direction of arrival (DOA), range and mutual coupling coefficient (MCC) are decoupled, thus only three one-dimensional (1-D) spectral searches are required to estimate the parameters of mixed rectilinear signals successively. Furthermore, the closed-form deterministic Cramer-Rao bound (CRB) of the concerned problem is also derived. Simulation results are provided to demonstrate the effectiveness of the proposed method for the classification and localization of mixed rectilinear sources.

Keywords:
DOA estimation, near-field, far-field, rectilinear signals, mutual coupling.

1. Introduction

As one representative application in numerous areas such as sonar, radar and wireless communications, the direction-of-arrival (DOA) estimation problem based on antenna arrays has drawn considerable attention [1–4]. Many high resolution algorithms [5–8] have been proposed for DOA estimation under the assumption of far-field (FF) signals (whose wavefronts are plane waves). However, in many interesting situations, the radiating sources are located close to the array, and thus called near-field (NF) signals (whose wavefronts are spherical waves), where both the DOA and range parameters need to be characterized. Consequently, traditional FF DOA estimation algorithms would be unreliable for NF source localization. Fortunately, various methods have been developed specifically for NF source localization [9–14]. Recently, simultaneous localization of both NF and FF signals has drawn a lot of attention in the array signal processing community given its many practical applications such as speaker localization using microphone arrays and guidance (homing) systems.

1.1. Related Work

In [15], Liang et al. proposed a two-stage MUSIC method based on two special fourth-order cumulant (FOC) matrices. By using FOC matrices, localization of mixed sources with sparse signal reconstruction was studied in [16,

Email addresses: dkchenhua0714@hotmail.com (Hua Chen), w.liu@sheffield.ac.uk (Wei Liu), weiping@ece.concordia.ca (Wei-Ping Zhu), swamy@ece.concordia.ca (M.N.S. Swamy), wangq@tju.edu.cn (Qing Wang)

17] and mixed-order MUSIC algorithms were proposed in [18–20], respectively. However, one common issue with these cumulant-based methods is their high computational complexity to construct FOC matrices. To avoid it, a series of second-order statistics (SOS)-based methods were presented in [21–23]. In [21], an oblique projection MUSIC-based algorithm was proposed to separate the NF and FF sources, which unfortunately yields extra estimation errors. As a result, Zuo et al. developed an alternating iterative method in [22] by recalculating the oblique projector without eigendecomposition. Resorting to the spatial differencing technique, a mixed localization method was presented in [23] by eliminating the FF and noise components from the covariance matrix of the array observation.

However, an ideal array manifold has been commonly assumed for all the abovementioned methods. In practice, an antenna array may have systematic errors, such as mutual coupling (MC) [24–26], gain and phase errors [27–30], etc., which will result in a tremendous degradation in parameter estimation performance. In particular, mutual coupling is a serious issue since in order to avoid phase ambiguities, all the abovementioned mixed source localization methods require the inter-sensor spacing to be constrained within a quarter wavelength, which inevitably results in the mutual coupling effect between closely located elements [24–26]. Mutual coupling is the electromagnetic interaction between the antenna elements in an array. The current developed in each antenna element of an array depends on their own excitation and also on the contributions from adjacent antenna elements. The mutual coupling effect can be considered as a kind of interference caused to the received antenna signal by neighboring antennas. Only in [31], a mixed source localization method was introduced in the presence of mutual coupling, but it would cause the array aperture loss problem when the principle of rank reduction (RARE) [45, 46] is used to decouple the FF DOAs and MC. The differencing RARE estimator adopted in [31] also has the array aperture loss problem in estimating the NF DOAs. When less array elements or strong MC presented, the method in [31] will fail to function.

On the other hand, strictly noncircular or rectilinear signals [32–40], including amplitude modulated (AM) and binary phase shift keying (BPSK) signals, are usually encountered in the context of radio communications, for which a significant gain in terms of DOA estimation performance can be achieved by taking into consideration both covariance matrix and conjugate covariance matrix of noncircular signals to expand the virtual array aperture. In [41–43], some rectilinearity-based methods are proposed to deal with the imperfect problem of array manifold in DOA estimation. But all of them have focused on FF DOA estimation only.

1.2. Contribution of the Paper

To the best of our knowledge, no work on rectilinearity-based localization of mixed NF and FF signals in the presence of unknown MC has been reported thus far. Therefore, in this paper, based on a uniform linear array (ULA), we propose a localization method for mixed NF and FF sources by exploiting the rectilinear information of the signals under unknown MC. By using the RARE principle, it is shown that only three one-dimensional (1-D) spectral searches are required to successively estimate the parameters of mixed NF and FF noncircular sources including DOA, range and mutual coupling coefficient (MCC). Meanwhile, distinguishing the types of sources is also solved without any extra processing. The main contributions of this paper are listed as follows.

1) To solve the aperture loss problem in [31], an extended new data model is constructed via stacking the original observed data and its conjugate counterpart under unknown MC to locate the mixed NF and FF signals based on rectilinearity. Instead of direct multiple dimensional (MD) searching method, a two-stage localization process is adopted. In the first stage, the FF DOAs are estimated with the extended noise subspace based on RARE principle, MC and FF noncircular phases are achieved with a unique eigenvector. In the second stage, based on twice RARE principle, the NF DOAs and ranges are decoupled with the estimated MC, and NF noncircular phases are estimated with another unique eigenvector.

2) We analyze the maximum number of incident mixed signals of the proposed method, which is more than that of the method in [31], to demonstrate the advantage of using the rectilinearity.

3) The computational complexity of the proposed method, direct MD searching method, the method by He et al. [21], and the method by Xie et al.[31] are analyzed. Our method gains the estimation performance at the expense of high complexity as compared to the He's method [21], and the Xie's method [31], but has better efficiency than the MD searching method by two-stage decoupling process.

4) The closed-form deterministic Cramer-Rao bound (CRB) of the concerned problem is derived to serve as the benchmark for performance assessment, whereas the CRB in [31] is only valid for the estimation of the circular signals.

1.3. Organization of the Paper

The rest of the paper is organized as follows. Section II describes the array signal model with mutual coupling. The proposed method is described in Section III, followed by the newly derived deterministic Cramer-Rao bound (CRB) in Section IV. The performance of our method is evaluated via computer simulations in Section V, and conclusions are drawn in Section VI.

Notations: $(\cdot)^*$, $(\cdot)^T$, $(\cdot)^H$, and $(\cdot)^{-1}$ represent operations of conjugation, transpose, conjugate transpose, and inverse, respectively; $E[\cdot]$ is the expectation operation; $arg(\cdot)$ is the phase operator of complex numbers; $diag\{\cdot\}$ stands for the diagonalization operation; $\mathbf{I}_p$ denotes the p-dimensional identity matrix; $\mathbf{1}_p$ denotes the p-dimensional row vector of 1s; $\mathbf{0}_{mn}$ denotes the $m \times n$ matrix of 0s; the $p \times p$ matrix $\mathbf{\Pi}_p$ is an exchange matrix with ones on its anti-diagonal and zeros elsewhere; $blkdiag\{\mathbf{Z}_1, \mathbf{Z}_2\}$ represents a block diagonal matrix with diagonal entries $\mathbf{Z}_1$ and $\mathbf{Z}_2$. $Re\{\cdot\}$ and $Im\{\cdot\}$ denote the real and imaginary parts, respectively, while $tr\{\cdot\}$, $vec\{\cdot\}$, and $\det[\cdot]$ denote the trace, vectorization and determinant of a matrix, respectively. $\otimes$ and $\odot$ are the Kronecker product and Hadamard product operations, respectively.

2. Array Signal Model

Similar to the scenario considered in [31], we suppose that there are K uncorrelated narrowband rectilinear sources $s_k(l)$ $(k = 1, 2, \dots, K; l = 1, 2, \dots, L)$ located in NF and FF regions, impinging onto a symmetric ULA with $M =$

$2N+1$ sensors. Here, l is the snapshot index and L is the total number of snapshots. A rectilinear signal can be represented as the product of a complex scalar $e^{j\psi/2}$ and a real valued signal $s_o(t)$. Without loss of generality, the first K_1 incoming sources $s_{N,k}(l)$ are assumed to be NF parameterized by (θ_k, r_k), where θ_k and r_k are the DOA of range and NF sources($k = 1, 2, \ldots, K_1$), while the remaining $K_2 = K - K_1$ sources $s_{F,k}(l)$ are FF parameterized by (θ_k, ∞) ($k = K_1+1, K_1+2, \ldots, K$), where K_1 and K_2 are known in advance. As pointed out in [15], an FF source can be considered as a special NF one where the range r_k approaches to ∞. With the array center indexed by 0 being the phase reference point, the lth snapshot of the array observed signal $\mathbf{x}(l) = [x_{-N}(l), \cdots, x_0(l), \cdots, x_N(l)]^T$ can be expressed in matrix form as

$$\begin{aligned}\mathbf{x}(l) &= \mathbf{A}_N\mathbf{s}_N(l) + \mathbf{A}_F\mathbf{s}_F(l) + \mathbf{n}(l)\\ &= \mathbf{A}\mathbf{s}(l) + \mathbf{n}(l)\end{aligned} \tag{1}$$

where $\mathbf{n}(l) = [n_{-N}(l), \cdots, n_0(l), \cdots, n_N(l)]^T$ represents the vector of circular Gaussian noise, with zero mean and variance σ_n^2, which is uncorrelated with the impinging signal, $\mathbf{s}(l) = \begin{bmatrix} \mathbf{s}_N^T(l) & \mathbf{s}_F^T(l) \end{bmatrix}^T$, $\mathbf{s}_N(l)$ and $\mathbf{s}_F(l)$ are the signal vectors of NF and FF sources, respectively, and $\mathbf{A} = \begin{bmatrix} \mathbf{A}_N & \mathbf{A}_F \end{bmatrix}$, $\mathbf{A}_N$ and $\mathbf{A}_F$ are the corresponding array steering matrices, composed of the steering vectors $\mathbf{a}_N(\theta_k, r_k)$ and $\mathbf{a}_F(\theta_k)$ at their kth column, respectively, i.e.,

$$\mathbf{A}_N = [\mathbf{a}_N(\theta_1, r_1), \cdots, \mathbf{a}_N(\theta_{K_1}, r_{K_1})] \tag{2}$$

with

$$\mathbf{a}_N(\theta_k, r_k) = [e^{j(-N\gamma_k + N^2\chi_k)}, \cdots, 1, \cdots, e^{j(N\gamma_k + N^2\chi_k)}]^T \tag{3}$$

$$\begin{aligned}\mathbf{A}_F &= [\mathbf{a}_N(\theta_{K_1+1}, \infty), \cdots, \mathbf{a}_N(\theta_K, \infty)]\\ &= [\mathbf{a}_F(\theta_{K_1+1}), \cdots, \mathbf{a}_F(\theta_K)]\end{aligned} \tag{4}$$

with

$$\mathbf{a}_F(\theta_k) = [e^{j(-N\gamma_k)}, \cdots, 1, \cdots, e^{j(N\gamma_k)}]^T \tag{5}$$

where $\gamma_k = -2\pi d\sin\theta_k/\lambda$ and $\chi_k = \pi d^2\cos^2\theta_k/(\lambda r_k)$ are called electric angles with λ being the wavelength of the incoming signal, $\theta_k \in \left[-\frac{\pi}{2}, \frac{\pi}{2}\right]$, $k = 1, \cdots K$, the DOA of the kth NF or FF signal, d the spacing between the sensors satisfying $d \le \lambda/4$ [14–23] and r_k the range of the kth NF signal that is within the Fresnel region [10, 11] and satisfies $r_k \in \left[0.62(D^3/\lambda)^{1/2}, 2D^2/\lambda\right]$, $k = 1, \cdots K_1$, with D being the array aperture.

With the rectilinearity of the signal, the signal vectors $\mathbf{s}_N(l)$ and $\mathbf{s}_F(l)$ can be expressed as [39, 40]

$$\mathbf{s}_N(l) = \boldsymbol{\psi}_{No}^{1/2}\mathbf{s}_{No}(l) \tag{6}$$

$$\mathbf{s}_F(l) = \boldsymbol{\psi}_{Fo}^{1/2}\mathbf{s}_{Fo}(l) \tag{7}$$

where $\mathbf{s}_{No}(l) = [s_{o,1}(l), \cdots, s_{o,K_1}(l)]^T$ and $\mathbf{s}_{Fo}(l) = [s_{o,K_1+1}(l), \cdots, s_{o,K}(l)]^T$ are the NF and FF real-valued signals, respectively. The diagonal matrices $\boldsymbol{\psi}_{No}^{1/2} = \boldsymbol{\psi}_N = diag(e^{j\psi_1/2}, \cdots, e^{j\psi_{K_1}/2})$ and $\boldsymbol{\psi}_{Fo}^{1/2} = \boldsymbol{\psi}_F = diag(e^{j\psi_{K_1+1}/2}, \cdots, e^{j\psi_K/2})$ are the arbitrary phase shifts corresponding to the NF and FF strictly non-circular sources $\mathbf{s}_N(l)$ and $\mathbf{s}_F(l)$, respectively.

In order to avoid phase ambiguities, the inter-element spacing d should be within a quarter wavelength, which will greatly increase the mutual coupling effect between the neighboring sensors. In the presence of mutual coupling, (1) should be modified into

$$\mathbf{x}(l)=\mathbf{C}\mathbf{A}_N\mathbf{s}_N(l)+\mathbf{C}\mathbf{A}_F\mathbf{s}_F(l)+\mathbf{n}(l) \tag{8}$$

where $\mathbf{C}$ denotes the $M\times M$ MCC matrix of the ULA, which is modeled as the following banded symmetric Toeplitz matrix with $P+1$ nonzero MCCs [24–26] as

$$\mathbf{C}=toeplitz(\mathbf{c},\mathbf{c}) \tag{9}$$

where $toeplitz(\cdot,\cdot)$ is the toeplitzation operation, and $\mathbf{c}=[1,\mathbf{c}_0^T]^T$, $\mathbf{c}_0=[c_1,c_2,\ldots,c_P]^T$.

3. The Proposed Method

The DOA estimation performance of traditional subspace methods based on (8) would degrade without compensating for mutual coupling. Thus, in this section, we develop a two-stage RARE-based DOA estimation method to determine the DOAs ($\theta_k, k=1,2,\cdots,K$) and ranges ($r_k, k=1,2,\cdots,K_1$) of the mixed NF and FF strictly noncircular sources under unknown mutual coupling. In the first stage, the FF DOAs are firstly decoupled by RARE under unknown mutual coupling. Second, the MCC matrix is reconstructed with the estimates of FF DOAs. In the second stage, by compensating for mutual coupling, the NF DOAs are decoupled though another RARE estimator based on the symmetry of the ULA. Finally, with the estimated NF DOAs, the range parameters of NF sources can be obtained through a third RARE estimator. The proposed method is described in detail in the following.

To exploit the noncircularity of the mixed incident signals, a new vector $\mathbf{z}(l)$ is constructed by stacking the observed data vector $\mathbf{x}(l)$ and its conjugate counterpart $\mathbf{x}^*(l)$ as follows

$$\begin{aligned}\mathbf{z}(l)&=\begin{bmatrix}\mathbf{x}(l)\\ \mathbf{x}^*(l)\end{bmatrix}\\ &=\mathbf{C}_e\mathbf{A}_{eN}\mathbf{s}_N(l)+\mathbf{C}_e\mathbf{A}_{eF}\mathbf{s}_F(l)+\mathbf{n}_e(l)\end{aligned} \tag{10}$$

where

$$\mathbf{C}_e=blkdiag\{\mathbf{C},\mathbf{C}^*\} \tag{11}$$

$$\begin{aligned}\mathbf{A}_{eN}&=\begin{bmatrix}\mathbf{A}_N\\ \mathbf{A}_N{}^*\boldsymbol{\psi}_N{}^*\end{bmatrix}\\ &=[\mathbf{a}_{eN}(\theta_1,r_1,\psi_1),\cdots,\mathbf{a}_{eN}(\theta_{K_1},r_{K_1},\psi_{K_1})]\end{aligned} \tag{12}$$

with

$$\mathbf{a}_{eN}(\theta_k,r_k,\psi_k)=\begin{bmatrix}\mathbf{a}_N(\theta_k,r_k)\\ \mathbf{a}_N{}^*(\theta_k,r_k)e^{-j\psi_k}\end{bmatrix} \tag{13}$$

$$\mathbf{A}_{eF} = \begin{bmatrix} \mathbf{A}_F \\ \mathbf{A}_F{}^* \boldsymbol{\psi}_F{}^* \end{bmatrix} = [\mathbf{a}_{eF}(\theta_{K_1+1}, \psi_{K_1+1}), \cdots, \mathbf{a}_{eF}(\theta_K, \psi_K)] \tag{14}$$

with

$$\mathbf{a}_{eF}(\theta_k, \psi_k) = \begin{bmatrix} \mathbf{a}_F(\theta_k) \\ \mathbf{a}_F{}^*(\theta_k) e^{-j\psi_k} \end{bmatrix} \tag{15}$$

$$\mathbf{n}_e(l) = \begin{bmatrix} \mathbf{n}(l) \\ \mathbf{n}^*(l) \end{bmatrix} \tag{16}$$

The covariance matrix of $\mathbf{z}(l)$ is written as

$$\begin{aligned} \mathbf{R} &= E[\mathbf{z}(l)\mathbf{z}^H(l)] \\ &= \mathbf{C}_e \mathbf{A}_{eN} \mathbf{R}_{sN} \mathbf{A}_{eN}^H \mathbf{C}_e^H + \mathbf{C}_e \mathbf{A}_{eF} \mathbf{R}_{sF} \mathbf{A}_{eF}^H \mathbf{C}_e^H + \sigma_n^2 \mathbf{I}_{2M} \end{aligned} \tag{17}$$

where $\mathbf{R}_{sN} = E[\mathbf{s}_N(l)\mathbf{s}_N^H(l)]$, $\mathbf{R}_{sF} = E[\mathbf{s}_F(l)\mathbf{s}_F^H(l)]$ and $\mathbf{R}_s = E[\mathbf{s}(l)\mathbf{s}^H(l)]$ are the covariance matrices of NF, FF and total mixed signals, respectively. The eigenvalue decomposition of $\mathbf{R}$ is given by

$$\mathbf{R} = \mathbf{U}_s \mathbf{\Lambda}_s \mathbf{U}_s^H + \mathbf{U}_n \mathbf{\Lambda}_n \mathbf{U}_n^H \tag{18}$$

where the $2M \times K$ matrix $\mathbf{U}_s$ and the $2M \times (2M-K)$ matrix $\mathbf{U}_n$ are the signal subspace and noise subspace, respectively. The $K \times K$ matrix $\mathbf{\Lambda}_s = diag\{\lambda_1, \lambda_2, \ldots, \lambda_K\}$ and the $(2M-K) \times (2M-K)$ matrix $\mathbf{\Lambda}_n = diag\{\lambda_{K+1}, \lambda_{K+2}, \ldots, \lambda_{2M}\}$ are diagonal matrices, where $\lambda_1 \geq \lambda_2 \geq \cdots \geq \lambda_K > \lambda_{K+1} = \cdots = \lambda_{2M} = \sigma_n^2$ are the eigenvalues of $\mathbf{R}$.

3.1. DOA Estimation of FF Sources and MCC Estimation

According to [25, 26], $\mathbf{C}\mathbf{a}_F(\theta)$ has an alternative expression as

$$\mathbf{C}\mathbf{a}_F(\theta) = \mathbf{T}_x(\theta)\mathbf{c} \tag{19}$$

where

$$\mathbf{T}_x(\theta) = \mathbf{T}_{x1}(\theta) + \mathbf{T}_{x2}(\theta) \tag{20}$$

$$[\mathbf{T}_{x1}(\theta)]_{i,j} = \begin{cases} [\mathbf{a}_F(\theta)]_{i+j-1} & i+j \leq M+1 \\ 0 & otherwise \end{cases} \tag{21}$$

$$[\mathbf{T}_{x2}(\theta)]_{i,j} = \begin{cases} [\mathbf{a}_F(\theta)]_{i-j+1} & i \geq j \geq 2 \\ 0 & otherwise \end{cases} \tag{22}$$

Obviously, based on the orthogonality between the noise subspace spanned by $\mathbf{U}_n$ and the signal subspace spanned by $\mathbf{U}_s$, the signal subspace can also be spanned by $\mathbf{C}_e\mathbf{A}_{eN}$ combined with $\mathbf{C}_e\mathbf{A}_{eF}$ jointly. Therefore, we have

$$\mathbf{U}_n^H \mathbf{C}_e \mathbf{a}_{eN}(\theta_k, r_k, \psi_k) = \mathbf{0}, k = 1, 2, \ldots, K^1. \tag{23}$$

[1]Becasuse an FF source can be considered as a special NF one where the range r_k approaches to ∞, (23) holds for both NF and FF sources.

$$\mathbf{U}_n^H \mathbf{C}_e \mathbf{a}_{eF}(\theta_k, \psi_k) = \mathbf{0}, k = K_1 + 1, K_1 + 2, \ldots, K. \tag{24}$$

In order to avoid multi-dimensional spectral search for estimating the DOA-range pairs, we can decouple the multi-parameters to reduce the computational load. First, FF DOA parameters are decoupled from other parameters. Substituting (11) and (15) into (24) and using (19), we obtain

$$\mathbf{U}_n^H \mathbf{T}(\theta_k)\zeta(\mathbf{c}, \psi_k) = \mathbf{0} \tag{25}$$

where $\mathbf{T}(\theta_k) = blkdiag\{\mathbf{T}_x(\theta_k), \mathbf{T}_x^*(\theta_k)\}$, $\zeta(\mathbf{c}, \psi_k) = \begin{bmatrix} \mathbf{c} \\ \mathbf{c}^* e^{-j\psi_k} \end{bmatrix}$. We now define a function $p_F(\theta)$ related to the DOA parameter as follows

$$p_F(\theta) = \{\det[\mathbf{Q}_F(\theta)]\}^{-1}. \tag{26}$$

where $\mathbf{Q}_F(\theta) = \mathbf{T}^H(\theta)\mathbf{U}_n\mathbf{U}_n^H\mathbf{T}(\theta)$.

Note that $\zeta(\mathbf{c}, \psi_k) \neq \mathbf{0}$, $\mathbf{U}_n^H \mathbf{T}(\theta_k)\zeta(\mathbf{c}, \psi_k) = \mathbf{0}$ holds for $k = K_1 + 1, K_1 + 2, \ldots, K$. Based on the RARE principle, if and only if $\theta = \theta_k, (k = K_1 + 1, \ldots, K)$, the matrix $\mathbf{Q}_F(\theta)$ is rank deficient or equivalently $\det[\mathbf{Q}_F(\theta)] = 0$. If searched over the confined region $\theta \in \left[-\frac{\pi}{2}, \frac{\pi}{2}\right]$, the DOA estimates of all FF sources could be obtained from the K_2 highest peaks.

Then, with the estimated DOA of FF sources, $\{\hat{\mathbf{c}}, \hat{\psi}_k\}$ can be obtained by finding the minima of the following function

$$\{\hat{\mathbf{c}}, \hat{\psi}_k\} = \min_{\mathbf{c},\psi} \zeta(\mathbf{c}, \psi)^H \mathbf{Q}_F(\hat{\theta})\zeta(\mathbf{c}, \psi), \tag{27}$$

which implies that $\zeta(\hat{\mathbf{c}}, \hat{\psi}_k)$ is just the unique eigenvector corresponding to the smallest eigenvalue of $\mathbf{Q}_F(\hat{\theta}_k)$, namely,

$$\hat{\zeta}_k = \zeta(\hat{\mathbf{c}}, \hat{\psi}_k) = \mathbf{e}_{min}[\mathbf{Q}_F(\hat{\theta}_k)], \mathbf{e}_{min}(1) = 1. \tag{28}$$

And we obtain the MCCs $\hat{\mathbf{c}}_0$ as

$$\hat{\mathbf{c}}_0 = \sum_{k=K_1+1}^{K} \hat{\zeta}_k(2 : P + 1)/(K - K_1) \tag{29}$$

and the noncircular phase estimate of FF sources as

$$\hat{\psi}_{F,k} = -arg(\hat{\zeta}_k(P + 2)) \tag{30}$$

The mutual coupling matrix $\hat{\mathbf{C}}$ can be reconstructed according to its banded symmetric Toeplitz structure in (9) with estimated MCCs.

3.2. DOA and Range Estimation of NF Sources

With estimated MCC, $\hat{\mathbf{C}}$ can be reconstructed to compensate for the mutual coupling in the NF source direction-finding process, and DOA and range estimation of NF sources can be obtained with (23).

Since the array is symmetric about the center sensor, (3) can be rewritten as

$$\mathbf{a}_N(\theta_k, r_k) = \mathbf{K}_N(\theta_k)\boldsymbol{\varsigma}_N(\theta_k, r_k) \tag{31}$$

Table 1: Summary of the proposed method

Input: L snapshots of the constructed array output vector, $\{\hat{\mathbf{z}}(l)\}_{l=1}^{L}$.
Output: DOA estimates $\hat{\theta}_k$ of all mixed NF and FF signals; range estimates $\hat{r}_k$ of NF signals; MCC estimates.
Stage 1: DOA estimation of FF sources and MCC estimation
1) Estimate the covariance matrix $\hat{\mathbf{R}} \approx \frac{1}{L}\sum_{l=1}^{L}\hat{\mathbf{z}}(l)\hat{\mathbf{z}}^H(l)$.
2) Perform subspace decomposition $\hat{\mathbf{R}} = \hat{\mathbf{U}}_s\hat{\mathbf{\Lambda}}_s\hat{\mathbf{U}}_s^H + \hat{\mathbf{U}}_n\hat{\mathbf{\Lambda}}_n\hat{\mathbf{U}}_n^H$ to get $\hat{\mathbf{U}}_n$.
3) Decouple $\mathbf{T}(\theta_k)$ related to FF sources under unknown mutual coupling.
4) Construct and search through $\hat{p}_F(\theta)$ to obtain DOAs $\hat{\theta}_k$ of FF signals based on the RARE principle.
5) Obtain MCC $\hat{\mathbf{c}}_0 = \sum_{k=K_1+1}^{K}\hat{\zeta}_k(2:P+1)/(K-K_1)$ with the estimated FF DOAs $\hat{\theta}_k$.
Stage 2: DOA and range estimation of NF sources
6) Reconstruct the extended MCC matrix $\hat{\mathbf{C}}_e$ with the estimated MCC $\hat{\mathbf{c}}_0$.
7) Construct and search through $\hat{p}_N(\theta)$ to obtain DOAs $\hat{\theta}_k$ of NF signals based on the RARE principle.
8) Construct and search through $\hat{p}_N(r)$ to obtain ranges $\hat{r}_k$ of NF signals with the estimated $\hat{\theta}_k$ using the RARE principle.

where $\mathbf{K}_N(\theta_k)$ is a $(2N+1)\times(N+1)$ matrix, whose elements depend only on the DOA parameter, i.e.,

$$\mathbf{K}_N(\theta_k)=\begin{bmatrix} \mathbf{V}_1^T(\theta_k) & \mathbf{v}_2^T(\theta_k) & \mathbf{V}_3^T(\theta_k) \end{bmatrix}^T \tag{32}$$

where

$$\mathbf{V}_1(\theta_k) = [\mathbf{P}_1(\theta_k), \mathbf{0}_{N\times 1}]_{N\times(N+1)} \tag{33}$$

with

$$\mathbf{P}_1(\theta_k) = diag\{e^{j(-N)\gamma_k}, e^{j(-N+1)\gamma_k}, ..., e^{-j\gamma_k}\} \tag{34}$$

$$\mathbf{v}_2(\theta_k) = [0, \ldots, 0, 1]_{1\times(N+1)} \tag{35}$$

$$\mathbf{V}_3(\theta_k) = [\mathbf{\Pi}_N\mathbf{P}_3(\theta_k), \mathbf{0}_{N\times 1}]_{N\times(N+1)} \tag{36}$$

with

$$\mathbf{P}_3(\theta_k) = diag\{e^{j(N)\gamma_k}, e^{j(N-1)\gamma_k}, ..., e^{j\gamma_k}\} \tag{37}$$

Meanwhile, $\boldsymbol{\varsigma}_N(\theta_k, r_k)$ is dependent on both the DOA and range parameters, as given by

$$\boldsymbol{\varsigma}_N(\theta_k, r_k) = [e^{j(-N)^2\chi_k}, e^{j(-N+1)^2\chi_k}, ..., 1]^T \tag{38}$$

Then, with (31), (23) can be rewritten as

$$\begin{aligned}\mathbf{0} &= \mathbf{U}_n^H\hat{\mathbf{C}}_e\mathbf{a}_{eN}(\theta_k, r_k, \psi_k)\\ &= \mathbf{U}_n^H\hat{\mathbf{C}}_e\mathbf{\Gamma}_N(\theta_k)\mathbf{\Upsilon}_N(\theta_k, r_k)\boldsymbol{\iota}_N(\psi_k)\end{aligned} \tag{39}$$

where

$$\boldsymbol{\Gamma}_N(\theta_k){=}blkdiag\{\mathbf{K}_N(\theta_k),\mathbf{K}_N^*(\theta_k)\} \tag{40}$$

$$\boldsymbol{\Upsilon}_N(\theta_k,r_k){=}blkdiag\{\boldsymbol{\varsigma}_N(\theta_k,r_k),\boldsymbol{\varsigma}_N^*(\theta_k,r_k)\} \tag{41}$$

$$\boldsymbol{\iota}_N(\psi_k){=}\begin{bmatrix} 1 \\ e^{-j\psi_k} \end{bmatrix} \tag{42}$$

We now define a function $p_N(\theta)$ that is related only to the DOA parameter as follows

$$p_N(\theta) = \{\det[\mathbf{Q}_{N1}(\theta)]\}^{-1}. \tag{43}$$

where $\mathbf{Q}_{N1}(\theta) = \boldsymbol{\Gamma}_N^H(\theta)\hat{\mathbf{C}}_e^H\mathbf{U}_n\mathbf{U}_n^H\hat{\mathbf{C}}_e\boldsymbol{\Gamma}_N(\theta)$. Similarly, notice that $\boldsymbol{\Upsilon}_N(\theta_k,r_k)\neq\mathbf{0}$, $\boldsymbol{\iota}_N(\psi_k)\neq\mathbf{0}$,

and $\mathbf{U}_n^H\hat{\mathbf{C}}_e\boldsymbol{\Gamma}_N(\theta_k)\boldsymbol{\Upsilon}_N(\theta_k,r_k)\boldsymbol{\iota}_N(\psi_k)=\mathbf{0}, k=1,2\ldots K',(K'\leq K)$.[2] Based on the RARE principle, the DOAs θ_k of all mixed signals can be obtained from the highest peaks of $p_N(\theta)$ over the confined region $\theta\in\left[-\frac{\pi}{2},\frac{\pi}{2}\right]$. Next, we substitute the estimated $\hat{\theta}_k$ from (43) into (39) and obtain the following function of the range parameter r:

$$p_N(r) = \{\det[\mathbf{Q}_{N2}(\hat{\theta}_k,r)]\}^{-1}. \tag{44}$$

where

$$\mathbf{Q}_{N2}(\hat{\theta}_k,r)=\boldsymbol{\Upsilon}_N^H(\hat{\theta}_k,r)\boldsymbol{\Gamma}_N^H(\hat{\theta}_k)\hat{\mathbf{C}}_e^H\mathbf{U}_n\mathbf{U}_n^H\hat{\mathbf{C}}_e\boldsymbol{\Gamma}_N(\hat{\theta}_k)\boldsymbol{\Upsilon}_N(\hat{\theta}_k,r).$$

Again, by searching for the range r over $\left[0.62(D^3/\lambda)^{1/2},2D^2/\lambda\right]$, the corresponding range of the NF signals can be obtained from the peaks of $p_N(r)$. If the range cannot be found in the Fresnel region with the estimated DOAs, then we can determine that the sources corresponding to the estimated DOAs are FF signals. It should be pointed out that the two-stage DOA estimation process introduced in Sec. 3.1 and 3.2 can identify the DOAs of FF sources by (26) and (43), respectively. But we use the first DOA estimator (26) to find the DOAs of FF sources, because the second DOA estimator (43) is based on the estimated extended $\hat{\mathbf{C}}_e$ in the first DOA estimation stage, which would cause error accumulation in estimating the DOAs of FF sources.

With the estimated DOA and range of NF sources, the noncircular phase $\hat{\psi}_{N,k}$ of NF sources can be achieved as

$$\hat{\boldsymbol{\iota}}_k=\boldsymbol{\iota}_N(\hat{\psi}_k)=\mathbf{e}_{min}[\mathbf{Q}_{N2}(\hat{\theta}_k,\hat{r}_k)],\mathbf{e}_{min}(1)=1. \tag{45}$$

$$\hat{\psi}_{N,k}=-arg(\hat{\iota}_k(2)) \tag{46}$$

The proposed method for mixed NF and FF strictly sources localization under mutual coupling is summarized in Table 1.

[2] Here, it should be pointed out that when some of the NF signals have the same DOAs as the FF signals, we only get K' DOAs which are no more than K true DOAs, namely $K'\leq K$.

Table 2: Computational complexity comparison for different methods.

Methods	Matrices construction	EVDs	Spectral searching
Xie[31]	$O\left((2N+1)^2L\right)$	$O\left(4/3(2N+1)^3\right)$	$O\left(2\frac{\pi}{\Delta\theta}(2N+1)^2 + K_1\frac{2D^2/\lambda-0.62(D^3/\lambda)^{1/2}}{\Delta r}(2N+1)^2\right)$
He[21]	$O\left((2N+1)^2L + (N+2)^2N\right)$	$O\left(4/3(2N+1)^3 + 4/3(N+2)^3\right)$	$O\left(\frac{\pi}{\Delta\theta}(2N+1)^2 + \frac{\pi}{\Delta\theta}(N+2)^2 + K_1\frac{2D^2/\lambda-0.62(D^3/\lambda)^{1/2}}{\Delta r}(2N+1)^2\right)$
Proposed	$O\left((4N+2)^2L\right)$	$O\left(4/3(4N+2)^3\right)$	$O\left(2\frac{\pi}{\Delta\theta}(4N+2)^2 + K_1\frac{2D^2/\lambda-0.62(D^3/\lambda)^{1/2}}{\Delta r}(4N+2)^2\right)$
MD searching	$O\left((4N+2)^2L\right)$	$O\left(4/3(4N+2)^3\right)$	$O\left(\frac{\pi}{\Delta\theta}\frac{2\pi}{\Delta\psi}(4N+2)^2 + \frac{\pi}{\Delta\theta}\frac{2D^2/\lambda-0.62(D^3/\lambda)^{1/2}}{\Delta r}\frac{2\pi}{\Delta\psi}(4N+2)^2\right)$

Remark 1: In practice, only a finite number of observed data samples are available. Thus, $\mathbf{R}$ is replaced by its finite-sample estimate

$$\hat{\mathbf{R}} \approx \frac{1}{L}\sum_{l=1}^{L}\hat{\mathbf{z}}(l)\hat{\mathbf{z}}^H(l). \tag{47}$$

Remark 2: In the proposed method, we have applied the RARE criterion to $\mathbf{Q}_F(\theta)$, $\mathbf{Q}_{N1}(\theta)$ and $\mathbf{Q}_{N2}(\hat{\theta}_k, r)$, respectively. According to the RARE criterion, if we have $2(2N+1) - K \geq 2(P+1)$, i.e., $K \leq 4N - 2P$, then $\mathbf{Q}_F(\theta)$ is in general of full rank. And if and only if the desired DOAs are obtained, the matrix $\mathbf{Q}_F(\theta)$ becomes rank deficient or equivalently $\det[\mathbf{Q}_F(\theta)] = 0$. Similarly, the conditions $K \leq 2N$ and $K \leq 4N$ should be satisfied for $\mathbf{Q}_{N1}(\theta)$ and $\mathbf{Q}_{N2}(\hat{\theta}_k, r)$, respectively. In summary, the number of incident mixed signals K for the proposed method should satisfy $K \leq min\{4N-2P, 2N\}$, while that of the method in [31] should satisfy $K \leq 2N - P$ and $K_1 \leq N$. Therefore, the proposed method can distinguish more signals than the method in [31], which can be demonstrated in Sec.5.1.

Remark 3: The computational complexity of the proposed method is compared with the direct MD spatial spectrum searching method, the He et al. method [21], and the Xie et al. method [31] in terms of the number of complex-valued multiplications, including the construction of $\hat{\mathbf{R}}$, performing EVD of $\hat{\mathbf{R}}$ and spectral searching. For comparison, we consider an array of $2N+1$ sensors for all the methods. Define the scanning interval for DOA $\theta \in \left[-\frac{\pi}{2}, \frac{\pi}{2}\right]$, range $r \in \left[0.62(D^3/\lambda)^{1/2}, 2D^2/\lambda\right]$ and noncircular phase $\psi \in [0, 2\pi]$ parameters as $\triangle\theta$, $\triangle r$ and $\triangle\psi$, respectively. The method of He et al. [21] involves constructing two covariance matrices with dimensions $(2N+1)\times(2N+1)$ and $(N+2)\times(N+2)$, performing EVDs of the two matrices, and executing spectral searching for DOA and range estimation. The method of Xie et al. [31] constructs a $(2N+1)\times(2N+1)$ covariance matrix, requires performing two EVDs as well as spectral searching for DOA and range estimation. For the proposed method, a $2(2N+1)\times 2(2N+1)$ covariance matrix is constructed, and one EVD is performed, followed by spectral searching for DOA and range estimation. The computational complexity comparison for these methods is summarized in Table 2, from which it can be concluded that the proposed method has much higher complexity than the methods in [21] and [31] due to the extended array aperture to improve the estimation accuracy, while it is more efficient than the MD searching method since it only need three 1-D searches.

4. Deterministic Rectilinear Cramer-Rao bound (CRB) under unknown mutual coupling

With the deterministic data assumption, a closed-form expression of the deterministic CRB for both DOA and range parameters of mixed sources is derived as an estimation benchmark for the scenario with mixed NF and FF strictly noncircular signals under unknown mutual coupling. The derivation is based on the Slepian-Bangs formula, and the result is summarized in the following theorem.

Theorem 1: Define a real-valued vector of the unknown parameters as $\boldsymbol{\xi} = \begin{bmatrix} \boldsymbol{\theta}_N^T & \mathbf{r}_N^T & \boldsymbol{\Psi}_N^T & \boldsymbol{\theta}_F^T & \boldsymbol{\Psi}_F^T & \mathbf{c}_R^T & \mathbf{c}_I^T & \mathbf{s}_o^T & \sigma_n^2 \end{bmatrix}^T$ with $\boldsymbol{\theta}_N = [\theta_1, \theta_2, ..., \theta_{K_1}]^T$, $\mathbf{r}_N = [r_1, r_2, ..., r_{K_1}]^T$, $\boldsymbol{\Psi}_N = [\psi_1, ..., \psi_{K_1}]^T$, $\boldsymbol{\theta}_F = [\theta_{K_1+1}, \theta_{K_1+2}, ..., \theta_K]^T$, $\boldsymbol{\Psi}_F = [\psi_{K_1+1}, ..., \psi_K]^T$, $\mathbf{c}_R = Re\{\mathbf{c}_0\}$, $\mathbf{c}_I = Im\{\mathbf{c}_0\}$ and $\mathbf{s}_o = [\mathbf{s}_o^T(1), \mathbf{s}_o^T(2), ..., \mathbf{s}_o^T(L)]^T$. We mainly focus on the interesting parameter vector $\boldsymbol{\varpi} = \begin{bmatrix} \boldsymbol{\theta}_N^T & \mathbf{r}_N^T & \boldsymbol{\Psi}_N^T & \boldsymbol{\theta}_F^T & \boldsymbol{\Psi}_F^T \end{bmatrix}^T$ and $\boldsymbol{\tau} = \begin{bmatrix} \mathbf{c}_R^T & \mathbf{c}_I^T \end{bmatrix}^T$. Resorting to the inversion formula of 3×3 block-partitioned matrices of

$$\mathbf{F} = \begin{bmatrix} \mathbf{F}_{\boldsymbol{\varpi}\boldsymbol{\varpi}} & \mathbf{F}_{\boldsymbol{\varpi}\boldsymbol{\tau}} & \mathbf{F}_{\boldsymbol{\varpi}\mathbf{s}_o} \\ \mathbf{F}_{\boldsymbol{\tau}\boldsymbol{\varpi}} & \mathbf{F}_{\boldsymbol{\tau}\boldsymbol{\tau}} & \mathbf{F}_{\boldsymbol{\tau}\mathbf{s}_o} \\ \mathbf{F}_{\mathbf{s}_o\boldsymbol{\varpi}} & \mathbf{F}_{\mathbf{s}_o\boldsymbol{\tau}} & \mathbf{F}_{\mathbf{s}_o\mathbf{s}_o} \end{bmatrix} \tag{48}$$

the deterministic CRB of $\boldsymbol{\varpi}$ and $\boldsymbol{\tau}$ for the mixed NF and FF strictly noncircular signals under unknown mutual coupling can be written respectively as

$$\begin{aligned} &\mathbf{C}^{nc}(\boldsymbol{\varpi}) \\ &= \Big(\mathbf{F}_{\boldsymbol{\varpi}\boldsymbol{\varpi}} - \mathbf{F}_{\boldsymbol{\varpi}\mathbf{s}_o}\mathbf{F}_{\mathbf{s}_o\mathbf{s}_o}^{-1}\mathbf{F}_{\mathbf{s}_o\boldsymbol{\varpi}} - \left(\mathbf{F}_{\boldsymbol{\varpi}\boldsymbol{\tau}} - \mathbf{F}_{\boldsymbol{\varpi}\mathbf{s}_o}\mathbf{F}_{\mathbf{s}_o\mathbf{s}_o}^{-1}\mathbf{F}_{\mathbf{s}_o\boldsymbol{\tau}}\right) \\ &\quad \times \left(\mathbf{F}_{\boldsymbol{\tau}\boldsymbol{\tau}} - \mathbf{F}_{\boldsymbol{\tau}\mathbf{s}_o}\mathbf{F}_{\mathbf{s}_o\mathbf{s}_o}^{-1}\mathbf{F}_{\mathbf{s}_o\boldsymbol{\tau}}\right)^{-1}\left(\mathbf{F}_{\boldsymbol{\tau}\boldsymbol{\varpi}} - \mathbf{F}_{\boldsymbol{\tau}\mathbf{s}_o}\mathbf{F}_{\mathbf{s}_o\mathbf{s}_o}^{-1}\mathbf{F}_{\mathbf{s}_o\boldsymbol{\varpi}}\right)\Big)^{-1} \end{aligned} \tag{49}$$

$$\begin{aligned} &\mathbf{C}^{nc}(\boldsymbol{\tau}) \\ &= \Big(\mathbf{F}_{\boldsymbol{\tau}\boldsymbol{\tau}} - \mathbf{F}_{\boldsymbol{\tau}\mathbf{s}_o}\mathbf{F}_{\mathbf{s}_o\mathbf{s}_o}^{-1}\mathbf{F}_{\mathbf{s}_o\boldsymbol{\tau}} - \left(\mathbf{F}_{\boldsymbol{\tau}\boldsymbol{\varpi}} - \mathbf{F}_{\boldsymbol{\tau}\mathbf{s}_o}\mathbf{F}_{\mathbf{s}_o\mathbf{s}_o}^{-1}\mathbf{F}_{\mathbf{s}_o\boldsymbol{\varpi}}\right) \\ &\quad \times \left(\mathbf{F}_{\boldsymbol{\varpi}\boldsymbol{\varpi}} - \mathbf{F}_{\boldsymbol{\varpi}\mathbf{s}_o}\mathbf{F}_{\mathbf{s}_o\mathbf{s}_o}^{-1}\mathbf{F}_{\mathbf{s}_o\boldsymbol{\varpi}}\right)^{-1}\left(\mathbf{F}_{\boldsymbol{\varpi}\boldsymbol{\tau}} - \mathbf{F}_{\boldsymbol{\varpi}\mathbf{s}_o}\mathbf{F}_{\mathbf{s}_o\mathbf{s}_o}^{-1}\mathbf{F}_{\mathbf{s}_o\boldsymbol{\tau}}\right)\Big)^{-1} \end{aligned} \tag{50}$$

where

$$\mathbf{F}_{\boldsymbol{\varpi}\boldsymbol{\varpi}} = \frac{2L}{\sigma_n^2} Re\{(\tilde{\mathbf{D}}^H \tilde{\mathbf{D}}) \odot \hat{\tilde{\mathbf{R}}}_s\} \tag{51}$$

$$\mathbf{F}_{\boldsymbol{\tau}\boldsymbol{\varpi}}^T = \mathbf{F}_{\boldsymbol{\varpi}\boldsymbol{\tau}} = \frac{2}{\sigma_n^2} \tilde{\check{\mathbf{S}}}_o^T (\mathbf{I}_L \otimes Re\{\tilde{\mathbf{D}}^H \tilde{\mathbf{C}}\}) \check{\mathbf{S}}_o \tag{52}$$

$$\mathbf{F}_{\mathbf{s}_o\boldsymbol{\varpi}}^T = \mathbf{F}_{\boldsymbol{\varpi}\mathbf{s}_o} = \frac{2}{\sigma_n^2} \tilde{\check{\mathbf{S}}}_o^T (\mathbf{I}_L \otimes Re\{\tilde{\mathbf{D}}^H \tilde{\mathbf{A}}\}) \tag{53}$$

$$\mathbf{F}_{\boldsymbol{\tau}\boldsymbol{\tau}} = \frac{2}{\sigma_n^2} \check{\mathbf{S}}_o^T (\mathbf{I}_L \otimes Re\{\tilde{\mathbf{C}}^H \tilde{\mathbf{C}}\}) \check{\mathbf{S}}_o \tag{54}$$

$$\mathbf{F}_{\mathbf{s}_o\boldsymbol{\tau}}^T = \mathbf{F}_{\boldsymbol{\tau}\mathbf{s}_o} = \frac{2}{\sigma_n^2} \check{\mathbf{S}}_o^T (\mathbf{I}_L \otimes Re\{\tilde{\mathbf{C}}^H \tilde{\mathbf{A}}\}) \tag{55}$$

$$\mathbf{F}_{\mathbf{s}_o\mathbf{s}_o} = \frac{2}{\sigma_n^2}\mathbf{I}_L \otimes Re\{\tilde{\mathbf{A}}^H\tilde{\mathbf{A}}\} \tag{56}$$

where $\tilde{\mathbf{D}} = [\tilde{\mathbf{D}}_{\theta N}, \tilde{\mathbf{D}}_{rN}, \tilde{\mathbf{D}}_{\psi N}, \tilde{\mathbf{D}}_{\theta F}, \tilde{\mathbf{D}}_{\psi F}] = [\mathbf{C}\mathbf{D}_{\theta N}\boldsymbol{\psi}_N, \mathbf{C}\mathbf{D}_{rN}\boldsymbol{\psi}_N, \frac{j}{2}\mathbf{C}\mathbf{A}_N\boldsymbol{\psi}_N, \mathbf{C}\mathbf{D}_{\theta F}\boldsymbol{\psi}_F, \frac{j}{2}\mathbf{C}\mathbf{A}_F\boldsymbol{\psi}_F]$,

$\mathbf{D}_{\theta N} = [\mathbf{d}_{\theta N}(\theta_1, r_1), \mathbf{d}_{\theta N}(\theta_2, r_2), \cdots, \mathbf{d}_{\theta N}(\theta_{K_1}, r_{K_1})]$ with $\mathbf{d}_{\theta N}(\theta_k, r_k) = \frac{\partial \mathbf{a}_N(\theta_k, r_k)}{\partial \theta_k}$,

$\mathbf{D}_{rN} = [\mathbf{d}_{rN}(\theta_1, r_1), \mathbf{d}_{rN}(\theta_2, r_2), \cdots, \mathbf{d}_{rN}(\theta_{K_1}, r_{K_1})]$ with $\mathbf{d}_{rN}(\theta_k, r_k) = \frac{\partial \mathbf{a}_N(\theta_k, r_k)}{\partial r_k}$, $\mathbf{D}_{\theta F} = [\mathbf{d}_{\theta F}(\theta_{K_1+1}), \mathbf{d}_{\theta F}(\theta_{K_1+2}), \cdots, \mathbf{d}_{\theta F}(\theta_K)]$ with $\mathbf{d}_{\theta F}(\theta_k) = \frac{\partial \mathbf{a}_F(\theta_k)}{\partial \theta_k}$, $\tilde{\mathbf{C}} = [1, j] \otimes [\tilde{\mathbf{D}}_{R,1}, \tilde{\mathbf{D}}_{R,2}, ..., \tilde{\mathbf{D}}_{R,P}]$ with $\tilde{\mathbf{D}}_{R,m} = \frac{\partial \mathbf{C}}{\partial \mathbf{c}_{R,m}}\mathbf{A}\boldsymbol{\psi}$, $\tilde{\mathbf{A}} = \mathbf{C}\mathbf{A}\boldsymbol{\psi}$, $\boldsymbol{\psi} = blkdiag\{\boldsymbol{\psi}_N, \boldsymbol{\psi}_F\}$,

$$\hat{\tilde{\mathbf{R}}}_s = \begin{bmatrix} \mathbf{1}_3 \otimes \mathbf{1}_3^T \otimes \hat{\mathbf{R}}_{\mathbf{S}_{No}\mathbf{S}_{No}}, \mathbf{1}_2 \otimes \mathbf{1}_3^T \otimes \hat{\mathbf{R}}_{\mathbf{S}_{No}\mathbf{S}_{Fo}} \\ \mathbf{1}_3 \otimes \mathbf{1}_2^T \otimes \hat{\mathbf{R}}_{\mathbf{S}_{No}\mathbf{S}_{Fo}}^T, \mathbf{1}_2 \otimes \mathbf{1}_2^T \otimes \hat{\mathbf{R}}_{\mathbf{S}_{Fo}\mathbf{S}_{Fo}} \end{bmatrix} \tag{57}$$

where $\hat{\mathbf{R}}_{\mathbf{S}_{No}\mathbf{S}_{No}} = \frac{1}{L}\mathbf{S}_{No}\mathbf{S}_{No}^T$, and $\hat{\mathbf{R}}_{\mathbf{S}_{Fo}\mathbf{S}_{Fo}} = \frac{1}{L}\mathbf{S}_{Fo}\mathbf{S}_{Fo}^T$ are the unconjugated covariance matrices of $\mathbf{S}_{No}$ and $\mathbf{S}_{Fo}$, respectively, $\hat{\mathbf{R}}_{\mathbf{S}_{No}\mathbf{S}_{Fo}} = \frac{1}{L}\mathbf{S}_{No}\mathbf{S}_{Fo}^T$ are the unconjugated cross covariance matrices of $\mathbf{S}_{No}$ and $\mathbf{S}_{Fo}$,

$$\tilde{\tilde{\mathbf{S}}}_o = \mathbf{J}_{(3K_1+2K_2)L} blkdiag\{\mathbf{I}_3 \otimes \tilde{\mathbf{S}}_{No}^T, \mathbf{I}_2 \otimes \tilde{\mathbf{S}}_{Fo}^T\} \tag{58}$$

where $\tilde{\mathbf{S}}_{No} = [\tilde{\mathbf{S}}_{No}(1), \tilde{\mathbf{S}}_{No}(2), ..., \tilde{\mathbf{S}}_{No}(L)]^T$ with $\tilde{\mathbf{S}}_{No}(l) = diag\{\mathbf{s}_{No}(l)\}$, $\tilde{\mathbf{S}}_{Fo} = [\tilde{\mathbf{S}}_{Fo}(1), \tilde{\mathbf{S}}_{Fo}(2), ..., \tilde{\mathbf{S}}_{Fo}(L)]^T$ with $\tilde{\mathbf{S}}_{Fo}(l) = diag\{\mathbf{s}_{Fo}(l)\}$, the commutation matrix $\mathbf{J}_{(3K_1+2K_2)L}$ has the form of

$$\mathbf{J}_{(3K_1+2K_2)L} = \begin{bmatrix} \mathbf{I}_L \otimes \mathbf{I}_{K_1}\mathbf{0}_{K_1(2K_1+2K_2)} \\ \mathbf{I}_L \otimes \mathbf{0}_{K_1K_1}\mathbf{I}_{K_1}\mathbf{0}_{K_1(K_1+2K_2)} \\ \mathbf{I}_L \otimes \mathbf{0}_{K_12K_1}\mathbf{I}_{K_1}\mathbf{0}_{K_12K_2} \\ \mathbf{I}_L \otimes \mathbf{0}_{K_23K_1}\mathbf{I}_{K_2}\mathbf{0}_{K_1K_2} \\ \mathbf{I}_L \otimes \mathbf{0}_{K_2(3K_1+K_2)}\mathbf{I}_{K_2}\mathbf{0}_{K_2K_2} \end{bmatrix}^T \tag{59}$$

$$\check{\mathbf{S}}_o = [\check{\mathbf{s}}_o^T(1), \check{\mathbf{s}}_o^T(2), ..., \check{\mathbf{s}}_o^T(L)]^T \tag{60}$$

where $\check{\mathbf{s}}_o(l) = \mathbf{I}_{2P} \otimes \mathbf{s}_o(l)$.

The proof of *Theorem 1* is given in Appendix A.

5. Simulation Results

In this section, the performance of the proposed method in localizing the mixed NF and FF strictly noncircular sources under unknown mutual coupling is compared with the He et al. method [21] and the Xie et al. method [31] as well as the deterministic CRB in *Theorem* 1 using a ULA with $d = \lambda/4$. For the first set of simulations, the ULA consists of $M = 7$ (or $N = 3$) sensors, while for the remaining set of simulations, the sensor number is $M = 9$ (or $N = 4$). The impinging sources are equi-power BPSK signals, and the additive noise is assumed to be spatially white complex Gaussian, and the SNR is defined relative to each signal. Further, as the MC effect is inversely proportional to the sensor distance, the nonzero MCCs are set to be [1, 0.3515+0.4656*i*, 0.0916-0.1218*i*]. The root mean square error (RMSE) of DOA and range parameters

$$\text{RMSE}(\vartheta_{K_i}) = \sqrt{\frac{1}{K_iM_c}\sum_{k=1}^{K_i}\sum_{q=1}^{M_c}(\hat{\vartheta}_{qk} - \vartheta_k)^2}, K_i = K_1, K_2,$$

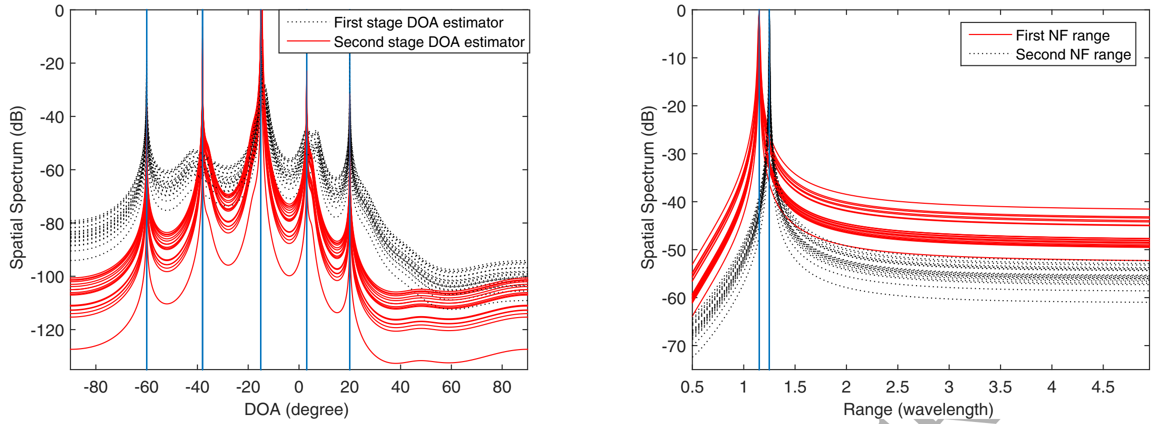

(a) (b)

Fig. 1: Spatial spectrum for the DOA and range estimation results.

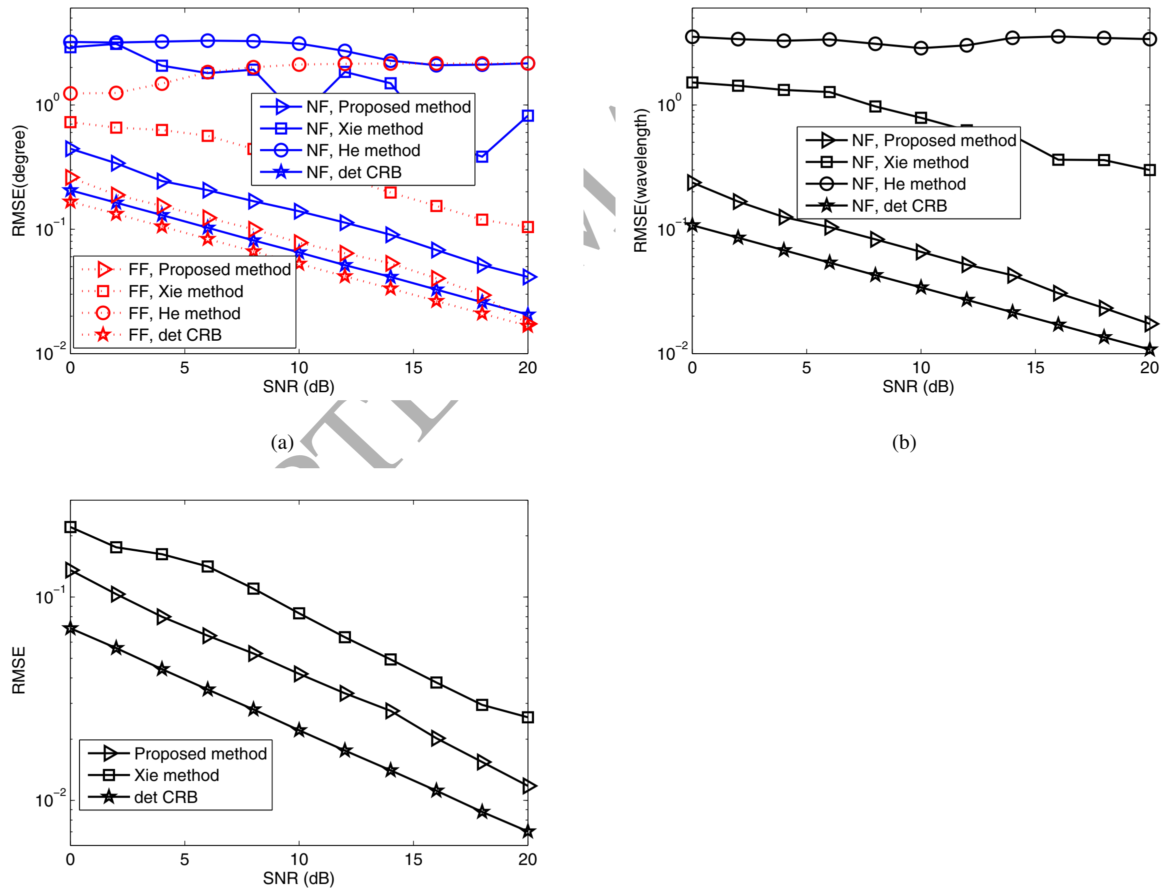

(a) (b)

(c)

Fig. 2: RMSE versus SNR for the DOA, range and MCC estimation results.

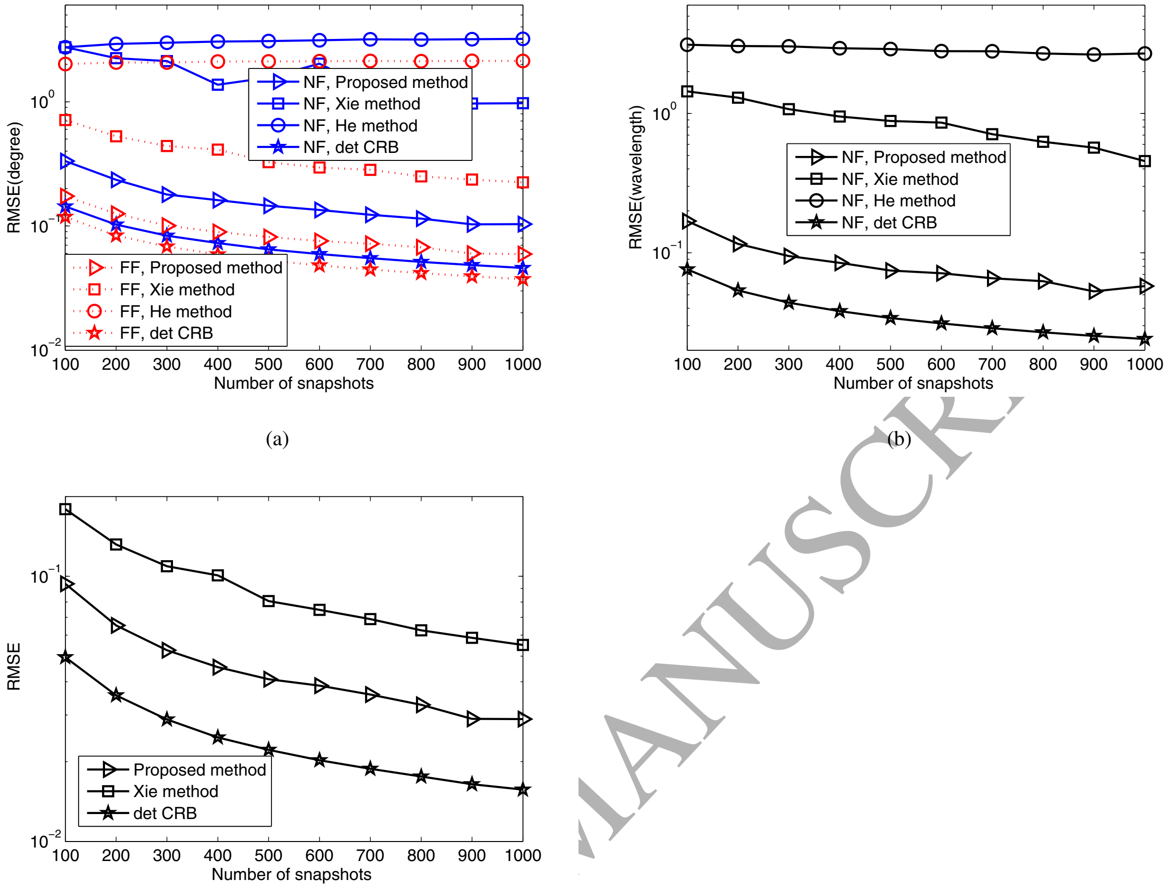

(a) (b) (c)

Fig. 3: RMSE versus snapshots for the DOA, range and MCC estimation results.

is adopted for quantitative evaluation, where M_c is the number of Monte Carlo simulations, K_i is the number of NF or FF signals, $\hat{\vartheta}_{q,k}$ is the estimate of the parameter $\hat{\theta}_k$ or $\hat{r}_k$ in the qth Monte Carlo simulation, and ϑ_k is the true value standing for either θ_k or r_k. The RMSE of estimated MCCs is defined as

$$\text{RMSE} = \sqrt{\frac{1}{M_c \, \|\mathbf{c}_0\|_2^2} \sum_{i=1}^{M_c} \left\|\hat{\mathbf{c}}_{0,i} - \mathbf{c}_0\right\|_2^2}$$

where $\hat{\mathbf{c}}_{0,i}$ is the estimated $\mathbf{c}_0$ in the ith Monte Carlo simulation, $\|\cdot\|_2$ denotes the Euclidean norm. The results of the first set of simulations are obtained from 20 independent Monte Carlo trials, and the remaining sets are from 500 independent Monte Carlo trials.

5.1. Spatial spectrum resolution

In the first set of simulations, two NF signals are located at $(-38°, 1.15\lambda)$, $(3°, 1.25\lambda)$, and three FF signals are located at $(-15°, +\infty)$, $(-60°, +\infty)$, $(20°, +\infty)$, respectively, which satisfies the number of incident mixed signals

$K_1 + K_2 = 5 \leq min\{4N - 2P, 2N\} = min\{8, 6\} = 6$. The SNR is 40 dB, and the number of snapshots is fixed at 500. The spatial spectrum resolution for DOA and range estimation is shown in Fig. 1(a)-(b). From Fig. 1(a), we can clearly see that only the DOAs of the FF sources can be identified in the first stage DOA estimation process, and after eliminating the mutual coupling effect, all the DOAs of mixed sources have been identified successfully since the FF source can be considered as a special NF one. From Fig. 1(b), only the range of the NF sources can be identified in the Fresnel region. Thus, we have successfully distinguished the types of mixed sources. However, the existing methods [21, 31] failed in this circumstance($K = 5 > 2N - P = 4$) because of the limited array aperture or uncompensated mutual coupling.

5.2. Performance versus SNR

In the second set of simulations, we investigate the RMSE of DOA, range and MCC estimates when the SNR varies from 0 dB to 20 dB, with the number of snapshots fixed at 500. Two NF signals are located at $(5°, 1.9\lambda)$, $(30°, 2.6\lambda)$, and two FF signals are located at $(5°, +\infty)$, $(-25°, +\infty)$, respectively. The RMSEs of DOA, range and MCC estimation are shown in Fig.2(a)-(c). In Fig. 2, it is obvious that the proposed method outperforms the methods in [21] and [31] for DOA estimation of both NF and FF sources, the range estimation as well as the MCC estimation. In addition, the RMSEs of the proposed method decrease monotonically as the SNR increases, and all the DOA, range and MCC estimation RMSEs are reasonably close to the corresponding CRBs. This is because the proposed method exploits the noncircular information of mixed signals, which increases the array aperture to some extent as compared to the methods in [21] and [31]. Furthermore, auto-calibration is adopted for the FF sources, while mutual coupling is compensated for the NF sources in the proposed method. However, as the SNR increases, the RMSEs of the He's method [21] remain uncharged, since the model error induced by mutual coupling is uncompensated.

5.3. Performance versus snapshots

In the third set of simulations, we examine the performance of the proposed method in comparison with the existing methods versus the number of snapshots. The simulation conditions are similar to those in the second example, except that the SNR is set at 10dB, and the number of snapshots varies from 100 to 1000. The results of DOA, range and MCC estimation are shown in Fig.3(a)-(c). As observed, as the number of snapshots increases, the proposed method is always superior to the existing ones in DOA, range and MCC estimation due to the use of noncircular information in mixed signals, and the RMSEs of DOA, range and MCC of the proposed method decrease monotonically and are close to the corresponding CRBs. The reason is that a better estimate of the covariance matrix can be obtained with a larger number of snapshots. While the mutual coupling effect is eliminated in the proposed method, the RMSEs of the He's method [21] remain almost constant due to it not being able to account for the mutual coupling effect.

5.4. Performance versus correlation factor

In the fourth set of simulations, we investigate the performance of the proposed method in comparison with the existing methods versus the correlation factor ρ varying from 0 to 0.95 between $s_1(t)$ and $s_4(t)$. The simulation

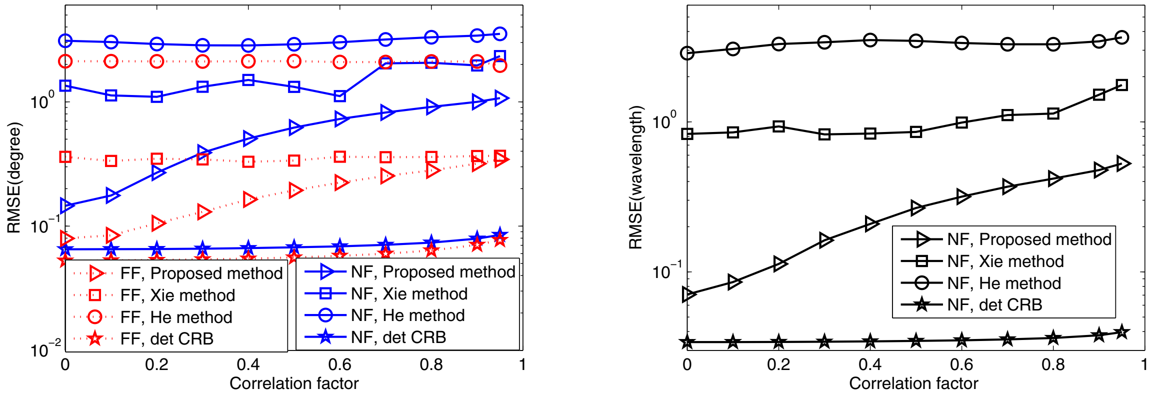

(a) (b)

Fig. 4: RMSE versus correlation factor for the DOA and range estimation results.

conditions are similar to those in the second example, except that the SNR is set at 10dB, and the number of snapshots is 500. The results of DOA and range estimation are shown in Fig.4(a)-(b). From the results in Fig.4, we can see that the proposed method significantly outperforms the methods in [21] and [31] in terms of DOA and range estimation, and as ρ increases, the correlation between $s_1(t)$ and $s_4(t)$ becomes strong, the RMSEs of the proposed method and Xie's method [31] becomes large. Therefore, the proposed method works only for independent or weakly correlated signals. On the contrary, the He's method [21] is completely failed to estimate the DOAs and ranges even in uncorrelated sources case due to the uncompensated mutual coupling.

6. Conclusion

We have presented an effective method for the localization of mixed FF and NF sources using the noncircular information of the impinging signals under unknown mutual coupling. Compared with the existing mixed source localization methods, the proposed one has its superiority under unknown mutual coupling and is capable of identifying source types reasonably. Moreover, high complexity multidimensional spectral search has been avoided in the proposed method by decoupling the array steering matrix of NF and FF signals. We have also derived the deterministic CRB of the problem under consideration as a benchmark. As demonstrated by simulation results, the proposed method is effective and outperforms two existing ones in the considered scenarios.

Appendix A. Proof of Theorem 1

Inspired by the analysis in [44], here we derive the CRB for the mixed NF and FF strictly noncircular sources under unknown mutual coupling by the Slepian-Bangs formulation. We first rewrite (8) with the support of (6), (7) as follows

$$\begin{aligned}\mathbf{x}(l) &= \mathbf{C}\mathbf{A}_N\boldsymbol{\psi}_N\mathbf{s}_{No}(l) + \mathbf{C}\mathbf{A}_F\boldsymbol{\psi}_F\mathbf{s}_{Fo}(l) + \mathbf{n}(l) \\ &= \mathbf{C}\mathbf{A}\boldsymbol{\psi}\mathbf{s}_o(l) + \mathbf{n}(l)\end{aligned} \tag{A.1}$$

where $\mathbf{s}_o(l)=\begin{bmatrix} \mathbf{s}_{No}^T(l) & \mathbf{s}_{Fo}^T(l) \end{bmatrix}^T$, and with L subsequent time samples, the observations can be modeled in matrix form as

$$\begin{aligned}\mathbf{X} &= \mathbf{C}\mathbf{A}_N\boldsymbol{\psi}_N\mathbf{S}_{No} + \mathbf{C}\mathbf{A}_F\boldsymbol{\psi}_F\mathbf{S}_{Fo} + \mathbf{N} \\ &= \mathbf{C}\mathbf{A}\boldsymbol{\psi}\mathbf{S}_o + \mathbf{N}\end{aligned} \tag{A.2}$$

where $\mathbf{X} = [\mathbf{x}(1), \mathbf{x}(2), ..., \mathbf{x}(L)]$, $\mathbf{S}_{No} = [\mathbf{s}_{No}(1), \mathbf{s}_{No}(2), ..., \mathbf{s}_{No}(L)]$, $\mathbf{S}_{Fo} = [\mathbf{s}_{Fo}(1), \mathbf{s}_{Fo}(2), ..., \mathbf{s}_{Fo}(L)]$, $\mathbf{S}_o = [\mathbf{s}_o(1), \mathbf{s}_o(2), ..., \mathbf{s}_o(L)]$ and $\mathbf{N} = [\mathbf{n}(1), \mathbf{n}(2), ..., \mathbf{n}(L)]$.

For convenience, we first vectorize the data model in (A.2) as follows

$$\begin{aligned}\mathbf{x} &= vec(\mathbf{X}) \\ &= (\mathbf{I}_L \otimes \mathbf{C}\mathbf{A}_N\boldsymbol{\psi}_N)\mathbf{s}_{No} + (\mathbf{I}_L \otimes \mathbf{C}\mathbf{A}_F\boldsymbol{\psi}_F)\mathbf{s}_{Fo} + \mathbf{n} \\ &= (\mathbf{I}_L \otimes \mathbf{C}\mathbf{A}\boldsymbol{\psi})\mathbf{s}_o + \mathbf{n}\end{aligned} \tag{A.3}$$

where $\mathbf{s}_{No} = vec\{\mathbf{S}_{No}\}$, $\mathbf{s}_{Fo} = vec\{\mathbf{S}_{Fo}\}$, $\mathbf{s}_o = vec\{\mathbf{S}_o\}$ and $\mathbf{n} = vec\{\mathbf{N}\}$. In (A.3), we have used the property that for arbitrary matrices $\mathbf{P}$, $\mathbf{B}$, and $\mathbf{X}$ of appropriate sizes, it holds that $vec\{\mathbf{PXB}\} = (\mathbf{B}^T \otimes \mathbf{P})vec\{\mathbf{X}\}$. To comply with the deterministic data assumption, the signal vectors $\mathbf{s}_0$ is assumed to be deterministic and unknown to the receiver, while the sensor noise $\mathbf{n}$ is zero-mean circularly symmetric white complex Gaussian distributed, and therefore, we have the mean $\boldsymbol{\varrho}$ and the covariance matrix $\boldsymbol{\Sigma}$ of the array output vector $\mathbf{x}$ as follows.

$$\begin{aligned}\boldsymbol{\varrho} &= (\mathbf{I}_L \otimes \mathbf{C}\mathbf{A}_N\boldsymbol{\psi}_N)\mathbf{s}_{No} + (\mathbf{I}_L \otimes \mathbf{C}\mathbf{A}_F\boldsymbol{\psi}_F)\mathbf{s}_{Fo} \\ &= (\mathbf{I}_L \otimes \mathbf{C}\mathbf{A}\boldsymbol{\psi})\mathbf{s}_o\end{aligned} \tag{A.4}$$

$$\boldsymbol{\Sigma} = \sigma_n^2\mathbf{I}_{LM} \tag{A.5}$$

The set of parameters that need to be considered for the deterministic CRB is then given by

$$\boldsymbol{\xi} = \begin{bmatrix} \boldsymbol{\theta}_N^T & \mathbf{r}_N^T & \boldsymbol{\Psi}_N^T & \boldsymbol{\theta}_F^T & \boldsymbol{\Psi}_F^T & \mathbf{c}_R^T & \mathbf{c}_I^T & \mathbf{s}_o^T & \sigma_n^2 \end{bmatrix}^T \tag{A.6}$$

where $\boldsymbol{\theta}_N = [\theta_1, \theta_2, ..., \theta_{K_1}]^T$, $\mathbf{r}_N = [r_1, r_2, ..., r_{K_1}]^T$, $\boldsymbol{\Psi}_N = [\psi_1, ..., \psi_{K_1}]^T$, $\boldsymbol{\theta}_F = [\theta_{K_1+1}, \theta_{K_1+2}, ..., \theta_K]^T$, $\boldsymbol{\Psi}_F = [\psi_{K_1+1}, ..., \psi_K]^T$, $\mathbf{c}_R = Re\{\mathbf{c}_0\}$, $\mathbf{c}_I = Im\{\mathbf{c}_0\}$ and $\mathbf{s}_o = [\mathbf{s}_o^T(1), \mathbf{s}_o^T(2), ..., \mathbf{s}_o^T(L)]^T$.

The principal parameter vector $\boldsymbol{\varpi} = \begin{bmatrix} \boldsymbol{\theta}_N^T & \mathbf{r}_N^T & \boldsymbol{\Psi}_N^T & \boldsymbol{\theta}_F^T & \boldsymbol{\Psi}_F^T \end{bmatrix}^T$ and $\boldsymbol{\tau} = \begin{bmatrix} \mathbf{c}_R^T & \mathbf{c}_I^T \end{bmatrix}^T$ are of interest to us, while the remaining ones are nuisance parameters.

The desired CRB matrix $\mathbf{C}^{nc}(\boldsymbol{\varpi})$ and $\mathbf{C}^{nc}(\boldsymbol{\tau})$for the mixed NF and FF strictly noncircular sources in the presence of unknown mutual coupling is usually computed by taking the inverse of the Fisher information matrix (FIM) $\mathbf{F}$ [44] for the parameter vector $\boldsymbol{\xi}$. In order to compute the FIM $\mathbf{F}$, the Slepian-Bangs formulation [44] can be applied if the data vector is Gaussian distributed. In this case, according to (A.4), the Slepian-Bangs formula is still valid for the deterministic data model in (A.3). The Slepian-Bangs formulation of $\mathbf{F}$ for the parameter vector $\boldsymbol{\xi}$ is given by [44]

$$\mathbf{F}_{\xi_p,\xi_q} = tr\left\{\boldsymbol{\Sigma}^{-1}\frac{\partial\boldsymbol{\Sigma}}{\partial\boldsymbol{\xi}_p}\boldsymbol{\Sigma}^{-1}\frac{\partial\boldsymbol{\Sigma}}{\partial\boldsymbol{\xi}_q}\right\} + 2Re\left\{(\frac{\partial\boldsymbol{\varrho}}{\partial\boldsymbol{\xi}_p})^H\boldsymbol{\Sigma}^{-1}\frac{\partial\boldsymbol{\varrho}}{\partial\boldsymbol{\xi}_q}\right\} \tag{A.7}$$

where $p, q = 1, \ldots, 3K_1 + 2K_2 + 2P + LK + 1$.

Since the covariance matrix $\boldsymbol{\Sigma}$ depends only on σ_n^2, the first part of (A.7) can be ignored. Therefore, (A.7) can be rewritten as

$$\mathbf{F}_{\xi_p,\xi_q} = 2Re\left\{(\frac{\partial \boldsymbol{\varrho}}{\partial \boldsymbol{\xi}_p})^H \boldsymbol{\Sigma}^{-1} \frac{\partial \boldsymbol{\varrho}}{\partial \boldsymbol{\xi}_q}\right\} \tag{A.8}$$

Then, the partial derivatives of $\boldsymbol{\varrho}$ with respect to the parameters $\boldsymbol{\theta}_N^T$, $\mathbf{r}_N^T$, $\boldsymbol{\Psi}_N^T$, $\boldsymbol{\theta}_F^T$, $\boldsymbol{\Psi}_F^T$ and $\mathbf{s}_o^T$ in (A.6) can be calculated directly as

$$\frac{\partial \boldsymbol{\varrho}}{\partial \boldsymbol{\theta}_N^T} = \left(\mathbf{I}_L \otimes \tilde{\mathbf{D}}_{\theta N}\right)\tilde{\mathbf{S}}_{No} \tag{A.9}$$

$$\frac{\partial \boldsymbol{\varrho}}{\partial \mathbf{r}_N^T} = \left(\mathbf{I}_L \otimes \tilde{\mathbf{D}}_{rN}\right)\tilde{\mathbf{S}}_{No} \tag{A.10}$$

$$\frac{\partial \boldsymbol{\varrho}}{\partial \boldsymbol{\Psi}_N^T} = j\left(\mathbf{I}_L \otimes \tilde{\mathbf{D}}_{\psi N}\right)\tilde{\mathbf{S}}_{No}/2 \tag{A.11}$$

$$\frac{\partial \boldsymbol{\varrho}}{\partial \boldsymbol{\theta}_F^T} = \left(\mathbf{I}_L \otimes \tilde{\mathbf{D}}_{\theta F}\right)\tilde{\mathbf{S}}_{Fo} \tag{A.12}$$

$$\frac{\partial \boldsymbol{\varrho}}{\partial \boldsymbol{\Psi}_F^T} = j\left(\mathbf{I}_L \otimes \tilde{\mathbf{D}}_{\psi F}\right)\tilde{\mathbf{S}}_{Fo}/2 \tag{A.13}$$

$$\frac{\partial \boldsymbol{\varrho}}{\partial \mathbf{s}_o^T} = \mathbf{I}_L \otimes \tilde{\mathbf{A}} \tag{A.14}$$

$$\frac{\partial \boldsymbol{\varrho}}{\partial \mathbf{c}_{R,m}} = (\mathbf{I}_L \otimes \tilde{\mathbf{D}}_{R,m})\mathbf{s}_o \tag{A.15}$$

$$\frac{\partial \boldsymbol{\varrho}}{\partial \mathbf{c}_{I,m}} = j(\mathbf{I}_L \otimes \tilde{\mathbf{D}}_{R,m})\mathbf{s}_o \tag{A.16}$$

It is easy to see that $\mathbf{F} = \mathbf{F}^T$. Consequently, we only need to compute the block matrices on and above the diagonal of $\mathbf{F}$. In the following derivation, we use the fact that for arbitrary vectors $\mathbf{a}$, $\mathbf{b}$, and a matrix $\mathbf{G}$, $diag\{\mathbf{a}\}\mathbf{G}diag\{\mathbf{b}\} = \mathbf{G} \odot (\mathbf{a}\mathbf{b}^T)$ holds. For the block matrices $\mathbf{F}_{\boldsymbol{\theta}_N,\boldsymbol{\theta}_N}$, $\mathbf{F}_{\boldsymbol{\theta}_N,r_N}$, $\mathbf{F}_{\boldsymbol{\theta}_N,\boldsymbol{\Psi}_N}$, $\mathbf{F}_{\boldsymbol{\theta}_N,\boldsymbol{\theta}_F}$, $\mathbf{F}_{\boldsymbol{\theta}_N,\boldsymbol{\Psi}_F}$, $\mathbf{F}_{\boldsymbol{\theta}_N,\mathbf{c}_{R,m}}$, $\mathbf{F}_{\boldsymbol{\theta}_N,\mathbf{c}_{I,m}}$, $\mathbf{F}_{\boldsymbol{\theta}_N,\mathbf{s}_o}$, $\mathbf{F}_{\mathbf{r}_N,\mathbf{r}_N}$, $\mathbf{F}_{\mathbf{r}_N,\boldsymbol{\Psi}_N}$, $\mathbf{F}_{\mathbf{r}_N,\boldsymbol{\theta}_F}$, $\mathbf{F}_{\mathbf{r}_N,\boldsymbol{\Psi}_F}$, $\mathbf{F}_{\mathbf{r}_N,\mathbf{c}_{R,m}}$, $\mathbf{F}_{\mathbf{r}_N,\mathbf{c}_{I,m}}$, $\mathbf{F}_{\mathbf{r}_N,\mathbf{s}_o}$, $\mathbf{F}_{\boldsymbol{\Psi}_N,\boldsymbol{\Psi}_N}$, $\mathbf{F}_{\boldsymbol{\Psi}_N,\boldsymbol{\theta}_F}$, $\mathbf{F}_{\boldsymbol{\Psi}_N,\boldsymbol{\Psi}_F}$, $\mathbf{F}_{\boldsymbol{\Psi}_N,\mathbf{c}_{R,m}}$, $\mathbf{F}_{\boldsymbol{\Psi}_N,\mathbf{c}_{I,m}}$, $\mathbf{F}_{\boldsymbol{\Psi}_N,\mathbf{s}_o}$, $\mathbf{F}_{\boldsymbol{\theta}_F,\boldsymbol{\theta}_F}$, $\mathbf{F}_{\boldsymbol{\theta}_F,\boldsymbol{\Psi}_F}$, $\mathbf{F}_{\boldsymbol{\theta}_F,\mathbf{c}_{R,m}}$, $\mathbf{F}_{\boldsymbol{\theta}_F,\mathbf{c}_{I,m}}$, $\mathbf{F}_{\boldsymbol{\theta}_F,\mathbf{s}_o}$, $\mathbf{F}_{\boldsymbol{\Psi}_F,\boldsymbol{\Psi}_F}$, $\mathbf{F}_{\boldsymbol{\Psi}_F,\mathbf{c}_{R,m}}$, $\mathbf{F}_{\boldsymbol{\Psi}_F,\mathbf{c}_{I,m}}$, $\mathbf{F}_{\boldsymbol{\Psi}_F,\mathbf{s}_o}$, $\mathbf{F}_{\mathbf{c}_{R,m},\mathbf{c}_{R,m}}$, $\mathbf{F}_{\mathbf{c}_{R,m},\mathbf{c}_{I,m}}$, $\mathbf{F}_{\mathbf{c}_{R,m},\mathbf{s}_o}$, $\mathbf{F}_{\mathbf{c}_{I,m},\mathbf{c}_{I,m}}$, and $\mathbf{F}_{\mathbf{c}_{I,m},\mathbf{s}_o}$, they can be obtained as

$$\begin{aligned}
&\mathbf{F}_{\boldsymbol{\theta}_N,\boldsymbol{\theta}_N} \\
&= \tfrac{2}{\sigma_n^2}\sum_{l=1}^{L} Re\left\{\tilde{\mathbf{S}}_{No}(l)\,\tilde{\mathbf{D}}_{\theta N}^H \tilde{\mathbf{D}}_{\theta N}\tilde{\mathbf{S}}_{No}(l)\right\} \\
&= \tfrac{2}{\sigma_n^2} Re\left\{\left(\tilde{\mathbf{D}}_{\theta N}^H \tilde{\mathbf{D}}_{\theta N}\right) \odot \sum_{l=1}^{L} \mathbf{s}_{No}(l)\,\mathbf{s}_{No}^T(l)\right\} \\
&= \tfrac{2L}{\sigma_n^2} Re\left\{\left(\tilde{\mathbf{D}}_{\theta N}^H \tilde{\mathbf{D}}_{\theta N}\right) \odot \tfrac{1}{L}\mathbf{S}_{No}\mathbf{S}_{No}^T\right\} \\
&= \tfrac{2L}{\sigma_n^2} Re\left\{\left(\tilde{\mathbf{D}}_{\theta N}^H \tilde{\mathbf{D}}_{\theta N}\right) \odot \hat{\mathbf{R}}_{\mathbf{S}_{No}\mathbf{S}_{No}}\right\}
\end{aligned} \tag{A.17}$$

$$\mathbf{F}_{\boldsymbol{\theta}_N,\mathbf{r}_N} = \frac{2L}{\sigma_n^2} Re\left\{\left(\tilde{\mathbf{D}}_{\theta N}^H \tilde{\mathbf{D}}_{rN}\right) \odot \hat{\mathbf{R}}_{\mathbf{S}_{No}\mathbf{S}_{No}}\right\} \tag{A.18}$$

$$\mathbf{F}_{\boldsymbol{\theta}_N,\boldsymbol{\Psi}_N} = \frac{2L}{\sigma_n^2} Re\left\{\left(\tilde{\mathbf{D}}_{\theta N}^H \tilde{\mathbf{D}}_{\psi N}\right) \odot \hat{\mathbf{R}}_{\mathbf{S}_{No}\mathbf{S}_{No}}\right\} \tag{A.19}$$

$$\mathbf{F}_{\boldsymbol{\theta}_N,\boldsymbol{\theta}_F} = \frac{2L}{\sigma_n^2} Re\left\{\left(\tilde{\mathbf{D}}_{\theta N}^H \tilde{\mathbf{D}}_{\theta F}\right) \odot \hat{\mathbf{R}}_{\mathbf{s}_{No}\mathbf{s}_{Fo}}\right\} \tag{A.20}$$

$$\mathbf{F}_{\boldsymbol{\theta}_N,\boldsymbol{\Psi}_F} = \frac{2L}{\sigma_n^2} Re\left\{\left(\tilde{\mathbf{D}}_{\theta N}^H \tilde{\mathbf{D}}_{\psi F}\right) \odot \hat{\mathbf{R}}_{\mathbf{s}_{No}\mathbf{s}_{Fo}}\right\} \tag{A.21}$$

$$\begin{aligned} &\mathbf{F}_{\boldsymbol{\theta}_N,\mathbf{c}_{R,m}} \\ &= \tfrac{2}{\sigma_n^2} Re\left\{\tilde{\mathbf{S}}_{No}^T \left(\mathbf{I}_L \otimes \tilde{\mathbf{D}}_{\theta N}^H\right)\left(\mathbf{I}_L \otimes \tilde{\mathbf{D}}_{R,m}\right)\mathbf{s}_o\right\} \\ &= \tfrac{2}{\sigma_n^2} Re\left\{\tilde{\mathbf{S}}_{No}^T \left(\mathbf{I}_L \otimes \left(\tilde{\mathbf{D}}_{\theta N}^H \tilde{\mathbf{D}}_{R,m}\right)\right)\mathbf{s}_o\right\} \\ &= \tfrac{2}{\sigma_n^2} \tilde{\mathbf{S}}_{No}^T \left(\mathbf{I}_L \otimes Re\left\{\tilde{\mathbf{D}}_{\theta N}^H \tilde{\mathbf{D}}_{R,m}\right\}\right)\mathbf{s}_o \end{aligned} \tag{A.22}$$

$$\mathbf{F}_{\boldsymbol{\theta}_N,\mathbf{c}_{I,m}} = \frac{2}{\sigma_n^2} \tilde{\mathbf{S}}_{No}^T \left(\mathbf{I}_L \otimes Re\left\{j\tilde{\mathbf{D}}_{\theta N}^H \tilde{\mathbf{D}}_{R,m}\right\}\right)\mathbf{s}_o \tag{A.23}$$

$$\mathbf{F}_{\boldsymbol{\theta}_N,\mathbf{s}_o} = \frac{2}{\sigma_n^2} \tilde{\mathbf{S}}_{No}^T \left(\mathbf{I}_L \otimes Re\left\{\tilde{\mathbf{D}}_{\theta N}^H \tilde{\mathbf{A}}\right\}\right) \tag{A.24}$$

$$\mathbf{F}_{\mathbf{r}_N,\mathbf{r}_N} = \frac{2L}{\sigma_n^2} Re\left\{\left(\tilde{\mathbf{D}}_{rN}^H \tilde{\mathbf{D}}_{rN}\right) \odot \hat{\mathbf{R}}_{\mathbf{s}_{No}\mathbf{s}_{No}}\right\} \tag{A.25}$$

$$\mathbf{F}_{\mathbf{r}_N,\boldsymbol{\Psi}_N} = \frac{2L}{\sigma_n^2} Re\left\{\left(\tilde{\mathbf{D}}_{rN}^H \tilde{\mathbf{D}}_{\psi N}\right) \odot \hat{\mathbf{R}}_{\mathbf{s}_{No}\mathbf{s}_{No}}\right\} \tag{A.26}$$

$$\mathbf{F}_{\mathbf{r}_N,\boldsymbol{\theta}_F} = \frac{2L}{\sigma_n^2} Re\left\{\left(\tilde{\mathbf{D}}_{rN}^H \tilde{\mathbf{D}}_{\theta F}\right) \odot \hat{\mathbf{R}}_{\mathbf{s}_{No}\mathbf{s}_{Fo}}\right\} \tag{A.27}$$

$$\mathbf{F}_{\mathbf{r}_N,\boldsymbol{\Psi}_F} = \frac{2L}{\sigma_n^2} Re\left\{\left(\tilde{\mathbf{D}}_{rN}^H \tilde{\mathbf{D}}_{\psi F}\right) \odot \hat{\mathbf{R}}_{\mathbf{s}_{No}\mathbf{s}_{Fo}}\right\} \tag{A.28}$$

$$\mathbf{F}_{\mathbf{r}_N,\mathbf{c}_{R,m}} = \frac{2}{\sigma_n^2} \tilde{\mathbf{S}}_{No}^T \left(\mathbf{I}_L \otimes Re\left\{\tilde{\mathbf{D}}_{rN}^H \tilde{\mathbf{D}}_{R,m}\right\}\right)\mathbf{s}_o \tag{A.29}$$

$$\mathbf{F}_{\mathbf{r}_N,\mathbf{c}_{I,m}} = \frac{2}{\sigma_n^2} \tilde{\mathbf{S}}_{No}^T \left(\mathbf{I}_L \otimes Re\left\{j\tilde{\mathbf{D}}_{rN}^H \tilde{\mathbf{D}}_{R,m}\right\}\right)\mathbf{s}_o \tag{A.30}$$

$$\mathbf{F}_{\mathbf{r}_N,\mathbf{s}_o} = \frac{2}{\sigma_n^2} \tilde{\mathbf{S}}_{No}^T \left(\mathbf{I}_L \otimes Re\left\{\tilde{\mathbf{D}}_{rN}^H \tilde{\mathbf{A}}\right\}\right) \tag{A.31}$$

$$\mathbf{F}_{\boldsymbol{\Psi}_N,\boldsymbol{\Psi}_N} = \frac{2L}{\sigma_n^2} Re\left\{\left(\tilde{\mathbf{D}}_{\psi N}^H \tilde{\mathbf{D}}_{\psi N}\right) \odot \hat{\mathbf{R}}_{\mathbf{s}_{No}\mathbf{s}_{No}}\right\} \tag{A.32}$$

$$\mathbf{F}_{\boldsymbol{\Psi}_N,\boldsymbol{\theta}_F} = \frac{2L}{\sigma_n^2} Re\left\{\left(\tilde{\mathbf{D}}_{\psi N}^H \tilde{\mathbf{D}}_{\theta F}\right) \odot \hat{\mathbf{R}}_{\mathbf{s}_{No}\mathbf{s}_{Fo}}\right\} \tag{A.33}$$

$$\mathbf{F}_{\boldsymbol{\Psi}_N,\boldsymbol{\Psi}_F} = \frac{2L}{\sigma_n^2} Re\left\{\left(\tilde{\mathbf{D}}_{\psi N}^H \tilde{\mathbf{D}}_{\psi F}\right) \odot \hat{\mathbf{R}}_{\mathbf{s}_{No}\mathbf{s}_{Fo}}\right\} \tag{A.34}$$

$$\mathbf{F}_{\boldsymbol{\Psi}_N,\mathbf{c}_{R,m}} = \frac{2}{\sigma_n^2} \tilde{\mathbf{S}}_{No}^T \left(\mathbf{I}_L \otimes Re\left\{\tilde{\mathbf{D}}_{\psi N}^H \tilde{\mathbf{D}}_{R,m}\right\}\right)\mathbf{s}_o \tag{A.35}$$

$$\mathbf{F}_{\boldsymbol{\Psi}_N,\mathbf{c}_{I,m}} = \frac{2}{\sigma_n^2} \tilde{\mathbf{S}}_{No}^T \left(\mathbf{I}_L \otimes Re\left\{j\tilde{\mathbf{D}}_{\psi N}^H \tilde{\mathbf{D}}_{R,m}\right\}\right)\mathbf{s}_o \tag{A.36}$$

$$\mathbf{F}_{\boldsymbol{\Psi}_N,\mathbf{s}_o} = \frac{2}{\sigma_n^2} \tilde{\mathbf{S}}_{No}^T \left(\mathbf{I}_L \otimes Re\left\{\tilde{\mathbf{D}}_{\psi N}^H \tilde{\mathbf{A}}\right\}\right) \tag{A.37}$$

$$\mathbf{F}_{\boldsymbol{\theta}_F,\boldsymbol{\theta}_F} = \frac{2L}{\sigma_n^2} Re\left\{\left(\tilde{\mathbf{D}}_{\theta F}^H \tilde{\mathbf{D}}_{\theta F}\right) \odot \hat{\mathbf{R}}_{\mathbf{s}_{Fo}\mathbf{s}_{Fo}}\right\} \tag{A.38}$$

$$\mathbf{F}_{\boldsymbol{\theta}_F,\boldsymbol{\Psi}_F} = \frac{2L}{\sigma_n^2} Re\left\{\left(\tilde{\mathbf{D}}_{\theta F}^H \tilde{\mathbf{D}}_{\psi F}\right) \odot \hat{\mathbf{R}}_{\mathbf{S}_{Fo}\mathbf{S}_{Fo}}\right\} \tag{A.39}$$

$$\mathbf{F}_{\boldsymbol{\theta}_F,\mathbf{c}_{R,m}} = \frac{2}{\sigma_n^2} \tilde{\mathbf{S}}_{Fo}^T \left(\mathbf{I}_L \otimes Re\left\{\tilde{\mathbf{D}}_{\theta F}^H \tilde{\mathbf{D}}_{R,m}\right\}\right) \mathbf{s}_o \tag{A.40}$$

$$\mathbf{F}_{\boldsymbol{\theta}_F,\mathbf{c}_{I,m}} = \frac{2}{\sigma_n^2} \tilde{\mathbf{S}}_{Fo}^T \left(\mathbf{I}_L \otimes Re\left\{j\tilde{\mathbf{D}}_{\theta F}^H \tilde{\mathbf{D}}_{R,m}\right\}\right) \mathbf{s}_o \tag{A.41}$$

$$\mathbf{F}_{\boldsymbol{\theta}_F,\mathbf{s}_o} = \frac{2}{\sigma_n^2} \tilde{\mathbf{S}}_{Fo}^T \left(\mathbf{I}_L \otimes Re\left\{\tilde{\mathbf{D}}_{\theta F}^H \tilde{\mathbf{A}}\right\}\right) \tag{A.42}$$

$$\mathbf{F}_{\boldsymbol{\Psi}_F,\boldsymbol{\Psi}_F} = \frac{2L}{\sigma_n^2} Re\left\{\left(\tilde{\mathbf{D}}_{\psi F}^H \tilde{\mathbf{D}}_{\psi F}\right) \odot \hat{\mathbf{R}}_{\mathbf{S}_{Fo}\mathbf{S}_{Fo}}\right\} \tag{A.43}$$

$$\mathbf{F}_{\boldsymbol{\Psi}_F,\mathbf{c}_{R,m}} = \frac{2}{\sigma_n^2} \tilde{\mathbf{S}}_{Fo}^T \left(\mathbf{I}_L \otimes Re\left\{\tilde{\mathbf{D}}_{\psi F}^H \tilde{\mathbf{D}}_{R,m}\right\}\right) \mathbf{s}_o \tag{A.44}$$

$$\mathbf{F}_{\boldsymbol{\Psi}_F,\mathbf{c}_{I,m}} = \frac{2}{\sigma_n^2} \tilde{\mathbf{S}}_{Fo}^T \left(\mathbf{I}_L \otimes Re\left\{j\tilde{\mathbf{D}}_{\psi F}^H \tilde{\mathbf{D}}_{R,m}\right\}\right) \mathbf{s}_o \tag{A.45}$$

$$\mathbf{F}_{\boldsymbol{\Psi}_F,\mathbf{s}_o} = \frac{2}{\sigma_n^2} \tilde{\mathbf{S}}_{Fo}^T \left(\mathbf{I}_L \otimes Re\left\{\tilde{\mathbf{D}}_{\psi F}^H \tilde{\mathbf{A}}\right\}\right) \tag{A.46}$$

$$\mathbf{F}_{\mathbf{c}_{I,m},\mathbf{c}_{I,m}} = \mathbf{F}_{\mathbf{c}_{R,m},\mathbf{c}_{R,m}} = \frac{2}{\sigma_n^2} \mathbf{s}_o^T \left(\mathbf{I}_L \otimes Re\left\{\tilde{\mathbf{D}}_{R,m}^H \tilde{\mathbf{D}}_{R,m}\right\}\right) \mathbf{s}_o \tag{A.47}$$

$$\mathbf{F}_{\mathbf{c}_{R,m},\mathbf{c}_{I,m}} = \frac{2}{\sigma_n^2} \mathbf{s}_o^T \left(\mathbf{I}_L \otimes Re\left\{j\tilde{\mathbf{D}}_{R,m}^H \tilde{\mathbf{D}}_{R,m}\right\}\right) \mathbf{s}_o \tag{A.48}$$

$$\mathbf{F}_{\mathbf{c}_{R,m},\mathbf{s}_o} = \frac{2}{\sigma_n^2} \mathbf{s}_o^T \left(\mathbf{I}_L \otimes Re\left\{\tilde{\mathbf{D}}_{R,m}^H \tilde{\mathbf{A}}\right\}\right) \tag{A.49}$$

$$\mathbf{F}_{\mathbf{c}_{I,m},\mathbf{s}_o} = -\frac{2}{\sigma_n^2} \mathbf{s}_o^T \left(\mathbf{I}_L \otimes Re\left\{j\tilde{\mathbf{D}}_{R,m}^H \mathbf{A}\right\}\right) \tag{A.50}$$

To proceed, we obtain the block matrices $\mathbf{F}_{\varpi\varpi}$, $\mathbf{F}_{\varpi\tau}$, $\mathbf{F}_{\varpi\mathbf{s}_o}$, $\mathbf{F}_{\tau\tau}$ and $\mathbf{F}_{\tau\mathbf{s}_o}$, respectively, as

$$\mathbf{F}_{\varpi\varpi} = \begin{bmatrix} \mathbf{F}_{\boldsymbol{\theta}_N,\boldsymbol{\theta}_N} & \mathbf{F}_{\boldsymbol{\theta}_N,\mathbf{r}_N} & \mathbf{F}_{\boldsymbol{\theta}_N,\boldsymbol{\Psi}_N} & \mathbf{F}_{\boldsymbol{\theta}_N,\boldsymbol{\theta}_F} & \mathbf{F}_{\boldsymbol{\theta}_N,\boldsymbol{\Psi}_F} \\ \mathbf{F}_{\mathbf{r}_N,\boldsymbol{\theta}_N} & \mathbf{F}_{\mathbf{r}_N,\mathbf{r}_N} & \mathbf{F}_{\mathbf{r}_N,\boldsymbol{\Psi}_N} & \mathbf{F}_{\mathbf{r}_N,\boldsymbol{\theta}_F} & \mathbf{F}_{\mathbf{r}_N,\boldsymbol{\Psi}_F} \\ \mathbf{F}_{\boldsymbol{\Psi}_N,\boldsymbol{\theta}_N} & \mathbf{F}_{\boldsymbol{\Psi}_N,\mathbf{r}_N} & \mathbf{F}_{\boldsymbol{\Psi}_N,\boldsymbol{\Psi}_N} & \mathbf{F}_{\boldsymbol{\Psi}_N,\boldsymbol{\theta}_F} & \mathbf{F}_{\boldsymbol{\Psi}_N,\boldsymbol{\Psi}_F} \\ \mathbf{F}_{\boldsymbol{\theta}_N,\boldsymbol{\theta}_N} & \mathbf{F}_{\boldsymbol{\theta}_N,\mathbf{r}_N} & \mathbf{F}_{\boldsymbol{\theta}_N,\boldsymbol{\Psi}_N} & \mathbf{F}_{\boldsymbol{\theta}_N,\boldsymbol{\theta}_F} & \mathbf{F}_{\boldsymbol{\theta}_N,\boldsymbol{\Psi}_F} \\ \mathbf{F}_{\boldsymbol{\Psi}_F,\boldsymbol{\theta}_N} & \mathbf{F}_{\boldsymbol{\Psi}_F,\mathbf{r}_N} & \mathbf{F}_{\boldsymbol{\Psi}_F,\boldsymbol{\Psi}_N} & \mathbf{F}_{\boldsymbol{\Psi}_F,\boldsymbol{\theta}_F} & \mathbf{F}_{\boldsymbol{\Psi}_F,\boldsymbol{\Psi}_F} \end{bmatrix} \tag{A.51}$$

$$\mathbf{F}_{\varpi\tau} = \begin{bmatrix} \mathbf{F}_{\boldsymbol{\theta}_N,\mathbf{c}_R} & \mathbf{F}_{\boldsymbol{\theta}_N,\mathbf{c}_I} \\ \mathbf{F}_{\mathbf{r}_N,\mathbf{c}_R} & \mathbf{F}_{\mathbf{r}_N,\mathbf{c}_I} \\ \mathbf{F}_{\boldsymbol{\Psi}_N,\mathbf{c}_R} & \mathbf{F}_{\boldsymbol{\Psi}_N,\mathbf{c}_I} \\ \mathbf{F}_{\boldsymbol{\theta}_N,\mathbf{c}_R} & \mathbf{F}_{\boldsymbol{\theta}_N,\mathbf{c}_I} \\ \mathbf{F}_{\boldsymbol{\Psi}_F,\mathbf{c}_R} & \mathbf{F}_{\boldsymbol{\Psi}_F,\mathbf{c}_I} \end{bmatrix} \tag{A.52}$$

$$\mathbf{F}_{\boldsymbol{\varpi}\mathbf{s}_o} = \begin{bmatrix} \mathbf{F}_{\boldsymbol{\theta}_N,\mathbf{s}_o} \\ \mathbf{F}_{\mathbf{r}_N,\mathbf{s}_o} \\ \mathbf{F}_{\boldsymbol{\Psi}_N,\mathbf{s}_o} \\ \mathbf{F}_{\boldsymbol{\theta}_N,\mathbf{s}_o} \\ \mathbf{F}_{\boldsymbol{\Psi}_F,\mathbf{s}_o} \end{bmatrix} \tag{A.53}$$

$$\mathbf{F}_{\boldsymbol{\tau\tau}} = \begin{bmatrix} \mathbf{F}_{\mathbf{c}_R,\mathbf{c}_R} & \mathbf{F}_{\mathbf{c}_R,\mathbf{c}_I} \\ \mathbf{F}_{\mathbf{c}_I,\mathbf{c}_R} & \mathbf{F}_{\mathbf{c}_I,\mathbf{c}_I} \end{bmatrix} \tag{A.54}$$

$$\mathbf{F}_{\boldsymbol{\tau}\mathbf{s}_o} = \begin{bmatrix} \mathbf{F}_{\mathbf{c}_R,\mathbf{s}_o} \\ \mathbf{F}_{\mathbf{c}_I,\mathbf{s}_o} \end{bmatrix} \tag{A.55}$$

After a simple derivation, the compact expression of (A.51)-(A.55) can be established immediately in (51)-(55).

Acknowledgement

This work is sponsored by Zhejiang Provincial Natural Science Foundation of China under Grant LQ19F010002, and by Natural Science Foundation of Ningbo Municipality under Grant No. 2018A610094, and by National Natural Science Foundation of China under Grant No. 61628101, 61871282 and 61571250, and by K.C.Wong Magna Fund in Ningbo University.

References

[1] H. Krim and M. Viberg, "Two decades of array signal processing research: The parametric approach," *IEEE Signal Process. Mag.*, vol. 13, no.4, pp. 67-94, 1996.

[2] R. O. Schmidt, "Multiple emitter location and signal parameter estimation," *IEEE Trans. Antennas Propaga.*, vol.34, no.3, pp.276-280, 1986.

[3] C. Zhou, Y. Gu, Z. Shi, and Y. D. Zhang, "Off-grid direction-of-arrival estimation using coprime array interpolation", *IEEE Signal Process. Lett.*, vol. 25, no. 11, pp. 1710-1714, Nov. 2018.

[4] X. F. Zhang, L. Y. Xu, L. Xu and D. Z. Xu, "Direction of departure (DOD) and direction of arrival (DOA) estimation in MIMO radar with reduced-dimension MUSIC," *IEEE Commun. Lett.*, vol. 14, no. 12, pp. 1161-1163, Dec. 2010.

[5] Q. Shen, W. Liu, W. Cui, S. L. Wu, Y. M. Zhang, and M. Amin, "Low-complexity direction-of-arrival estimation based on wideband co-prime arrays," *IEEE Trans. Audio, Speech and Language Process.*, vol. 23, no. 9, pp. 1445-1456, Sep. 2015.

[6] X. Wu, W.-P. Zhu, and J. Yan, "A Toeplitz covariance matrix reconstruction approach for direction-of-arrival estimation," *IEEE Trans. Veh. Technol.*,vol. 66, no. 9, pp. 8223-8237, Sept. 2017.

[7] J. F. Gu, W.-P. Zhu, and M. N. S. Swamy, "Direction of arrival tracking for signals with known waveforms based on block least squares techniques." *Journal of the Franklin Institute*, vol. 354, no. 11, pp. 4573-4594, Dec. 2017.

[8] C. Zhou, Y. Gu, X. Fan, Z. Shi, G. Mao and Y. D. Zhang, "Direction-of-arrival estimation for coprime array via virtual array interpolation," *IEEE Trans. Signal Process.*, vol. 66, no. 22, pp. 5956-5971, Nov. 2018.

[9] X. F. Zhang, W. Y. Chen, W. Zheng, et al., "Localization of near-field sources: a reduced-dimension MUSIC algorithm," *IEEE Commun. Lett.*, vol. 22, no. 7, pp. 1422-1425, Jul. 2018.

[10] Y. Wu, H. C. So, and J. Li, "Passive localization of near-field sources with a polarization sensitive array," *IEEE Trans. Antenna Propag.*, vol. 55, no. 8, pp. 2402-2408, Aug. 2007.

[11] J. W. Tao, L. Liu, and Z. Y. Lin, "Joint DOA, range, and polarization estimation in the Fresnel region," *IEEE Trans. Aerosp. Electron. Syst.*, vol. 47, no. 4, pp. 2657-2672, Oct. 2011.

[12] J. He, M. O. Ahmad, and M. N. S. Swamy, "Near-Field localization of partially polarized sources with a cross-dipole array," *IEEE Trans. Aerosp. Electron. Syst.*, vol. 49, no. 2, pp. 857-870, Apr. 2013.

[13] E. Grosicki, K. Abed-Meraim, and Y. Hua, "A weighted linear prediction method for near-field source localization," *IEEE Trans. Signal Process.*, vol. 53, no. 10, pp. 3651-3660, Oct. 2005.

[14] W. Zhi and M. Y. W. Chia, "Near-field source localization via symmetric subarrays," *IEEE Signal Process. Lett.*, vol. 14, no. 6, pp. 409-412, Jun. 2007.

[15] J. Liang and D. Liu, "Passive localization of mixed near-field and far-field sources using two-stage MUSIC algorithm," *IEEE Trans. Signal Process.*, vol. 58, no. 1, pp. 108-120, Jan. 2010.

[16] B. Wang, J. Liu and X. Sun, "Mixed sources localization based on sparse signal reconstruction," *IEEE Signal Process. Lett.*, vol. 19, no. 8, pp. 487-490, Aug. 2012.

[17] Y. Tian, Q.S. Lian, H. Xu, "Mixed near-field and far-field source localization utilizing symmetric nested array," *Digit. Signal Process.*, vol.73, pp. 16-23, Feb. 2018.

[18] Z. Zheng, J. Sun, W. Q. Wang, et al. "Classification and localization of mixed near-field and far-field sources using mixed-order statistics," *Signal Process.*, vol.143, pp.134-139, Feb.2018.

[19] B. Wang, Y. Zhao and J. Liu, "Mixed-order MUSIC algorithm for localization of far-field and near-field sources," *IEEE Signal Process. Lett.*, vol. 20, no. 4, pp. 311-314, Apr. 2013.

[20] Z. Zheng, M. Fu, W. Q. Wang, et al. "Mixed far-field and near-field source localization based on subarray cross-cumulant," *Signal Process.*, vol.150, pp. 51-56, Sep.2018.

[21] J. He, M. N. S. Swany, and M. O. Ahmad, "Efficient application of MUSIC algorithm under the coexistence of far-field and near-field sources," *IEEE Trans. Signal Process.*, vol. 60, no. 4, pp. 2066-2070, Apr. 2012.

[22] W. Zuo, J. Xin, J. Wang, N. Zheng and A. Sano, "A computationally efficient source localization method for a mixture of near-field and far-field narrowband signals," in *Proc. IEEE Int. Conf. Acoust., Speech, Signal Process. (ICASSP)*, Florence, 2014, pp. 2257-2261.

[23] G. Liu and X. Sun, "Spatial differencing method for mixed far-field and near-field sources localization," *IEEE Signal Process. Lett.*, vol.21, no.11, pp. 1331-1335, 2014.

[24] B. Liao, Z. G. Zhang and S. C. Chan, "DOA estimation and tracking of ULAs with mutual coupling," *IEEE Trans. Aerosp. Electron. Syst.*, vol. 48, no. 1, pp. 891-905, Jan. 2012.

[25] Z. Ye, J. Dai, X. Xu and X. Wu, "DOA estimation for uniform linear array with mutual coupling," *IEEE Trans. Aerosp. Electron. Syst.*, vol. 45, no. 1, pp. 280-288, Jan. 2009.

[26] Z. Ye and C. Liu, "On the resiliency of MUSIC direction finding against antenna sensor coupling," *IEEE Trans. Antenna Propag.*, vol. 56, no. 2, pp. 371-380, Feb. 2008.

[27] W. Wang, R. Wu, J. Liang and H. C. So, "Phase retrieval approach for DOA estimation with array errors," *IEEE Trans. Aerosp. Electron. Syst.*, vol. 53, no. 5, pp. 2610-2620, Oct. 2017.

[28] J. Liu, X. Wu, W. J. Emery, et al. "Direction-of-Arrival estimation and sensor array error calibration based on blind signal separation," *IEEE Signal Process. Lett.*, vol. 24, no. 1, pp. 7-11, Jan. 2017.

[29] S. Cao, Z. Ye, D. Xu and X. Xu, "A Hadamard product based method for DOA estimation and gain-phase error calibration," *IEEE Trans. Aerosp. Electron. Syst.*, vol. 49, no. 2, pp. 1224-1233, Apr. 2013.

[30] A. Liu, G. Liao, C. Zeng, Z. Yang and Q. Xu, "An eigenstructure method for estimating DOA and sensor gain-phase errors," *IEEE Trans. Signal Process.*, vol. 59, no. 12, pp. 5944-5956, Dec. 2011.

[31] J. Xie, H. Tao, X. Rao and J. Su, "Localization of mixed far-field and near-field sources under unknown mutual coupling," *Digital Signal Process.*, vol. 50, pp. 229-239, 2016.

[32] H. Abeida, J.P. Delmas, "Statistical performance of MUSIC-like algorithms in resolving noncircular sources," *IEEE Trans. Signal Process.*,

vol. 56, no. 9, pp. 4317-4329, Sep. 2008.

[33] H. Chen, C. P. Hou, W.-P. Zhu, W. Liu, Y. Y. Dong, Z.J. Peng and Q. Wang. "ESPRIT-like two-dimensional direction finding for mixed circular and strictly noncircular sources based on joint diagonalization," *Signal Process.*, vol.141, pp.48-56, Dec.2017.

[34] H. Abeida and J. P. Delmas, "Direct derivation of the stochastic CRB of DOA estimation for rectilinear sources," *IEEE Signal Process. Lett.*, vol. 24, no. 10, pp. 1522-1526, Oct. 2017.

[35] Y. Yue, Y. Xu, Z. Liu and L. Shen, "Parameter estimation of coexisted circular and strictly noncircular sources using diversely polarized antennas," *IEEE Commun. Lett.*, vol. 22, no. 9, pp. 1822-1825, Sep. 2018.

[36] Y. Shi, L. Huang, C. Qian, and H.C. So, "Direction-of-arrival estimation for noncircular sources via structured least squares-based esprit using three-axis crossed array," *IEEE Trans. Aerosp. Electron. Syst.*, vol. 51, no. 2, pp. 1267-1278, 2015.

[37] H. Chen, W.-P. Zhu, W. Liu, et al. "RARE-based localization for mixed near-field and far-field rectilinear sources," *Digit. Signal Process.*, 2018.

[38] J. Steinwandt, F. Roemer, M. Haardt, and G. Del Galdo, "R-dimensional ESPRIT-type algorithms for strictly second-order non-circular sources and their performance analysis," *IEEE Trans. Signal Process.*, vol. 62, no. 18, pp. 4824-4838, Sept. 2014.

[39] Z.-M. Liu, Z.-T. Huang, Y.-Y. Zhou, and J. Liu, "Direction-of-arrival estimation of noncircular signals via sparse representation," *IEEE Trans. Aerosp. Electron. Syst.*, vol. 48, no. 3, pp. 2690–2698, 2012.

[40] H. Chen, C. P. Hou, W. Liu, W.-P. Zhu, and M.N.S. Swamy. "Efficient two-dimensional direction of arrival estimation for a mixture of circular and noncircular sources," *IEEE Sensors J.*, vol. 16, no. 8, pp. 2527-2536, Apr. 2016.

[41] W. Xie, C. Wang, F. Wen, et al. "DOA and gain-phase errors estimation for noncircular sources with central symmetric array," *IEEE Sensors J.*, vol. 17, no. 10, pp. 3068-3078, May. 2017.

[42] S. Cao, D. Xu, X. Xu and Z. Ye, "DOA estimation for noncircular signals in the presence of mutual coupling," *Signal Process.*, vol. 105, pp. 12–16, 2014.

[43] H. Huang, B. Liao, Guo X, et al. "DOA estimation of rectilinear signals with a partly calibrated uniform linear array," *Signal Process.*, vol.147, pp.203-207, Jun. 2018.

[44] D. M. Kitavi, K. T. Wong and C. C. S. Hung, "An L-Shaped array with non-orthogonal axes-its cramér-rao bound for direction finding," *IEEE Trans. Aerosp. Electron. Syst.*, vol. 54, no.1, pp. 486-492, Feb. 2018.

[45] A. Ferreol, E. Boyer and P. Larzabal, "Low-cost algorithm for some bearing estimation methods in presence of separable nuisance parameters," *Electron. Lett.*, vol. 40, no. 15, pp. 966-967, Jul. 2004.

[46] M. Pesavento, A. B. Gershman and K. M. Wong, "Direction finding in partly calibrated sensor arrays composed of multiple subarrays," *IEEE Trans. Signal Process.*, vol. 50, no. 9, pp. 2103-2115, Sep. 2002.